Brain Tumor Detection and Classification using Novel Image Segmentation Approach for MRI Images

Research Scholar

Ms. Bhavna K Pancholi

Guide

Dr. Pramod S Modi

❖ CONTENTS

1. MOTIVATION AND INTRODUCTION

- High risk factor with abnormal growth of brain tumor cells
- Brain tumor detection and classification is highly recommended for medical diagnosis and treatment
- Machine learning approach for brain tumor detection and classification
- Modalities (MRI, CT scan, etc.)
- Types of Tumors - Benign and Malignant

2. GENERAL BLOCK DIAGRAM OF THE IMAGE DETECTION AND CLASSIFICATION

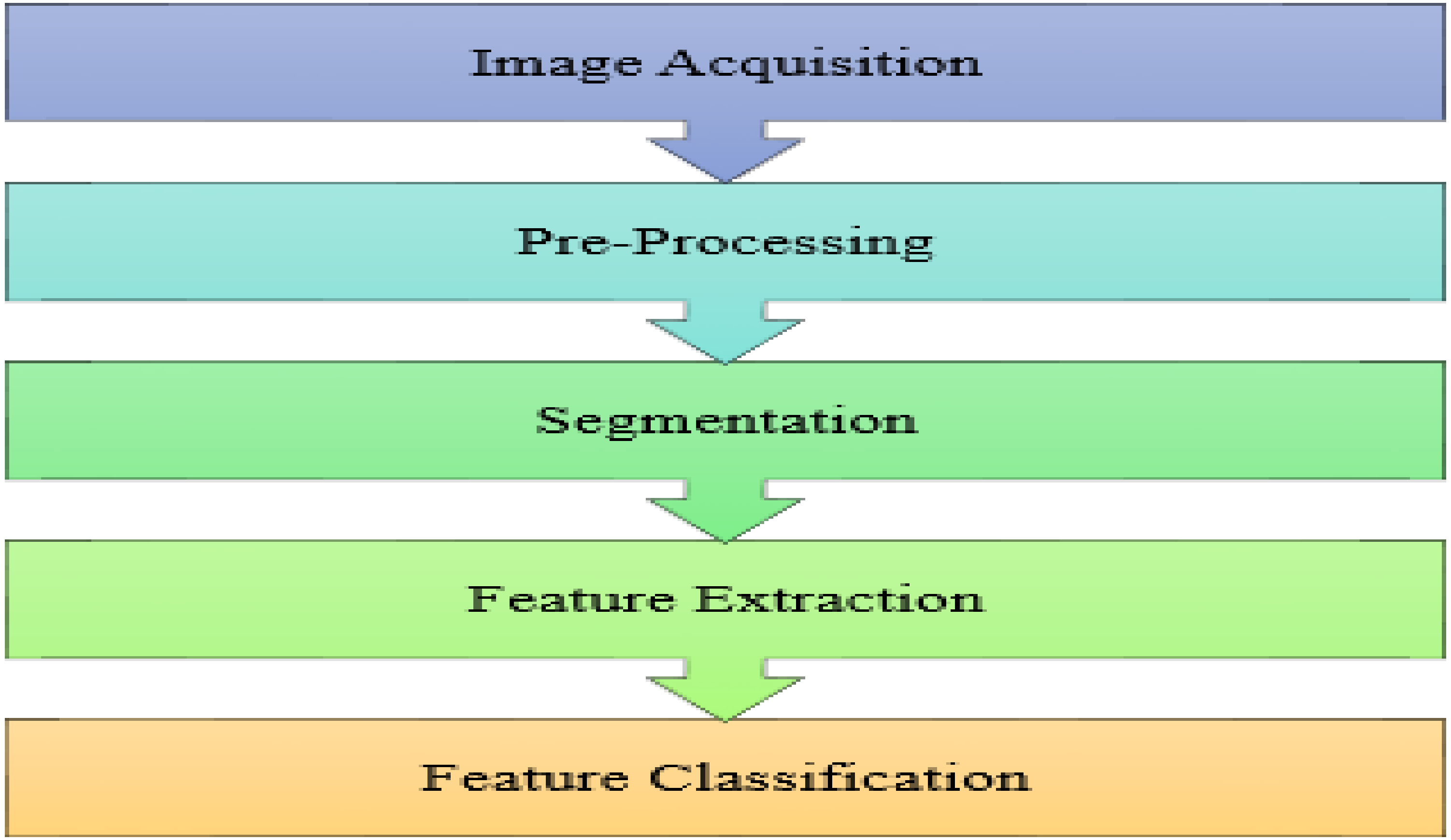

3. LITERATURE REVIEW

1) Image Modalities

- CT-Scan [5,18]
- X-RAY [5,18]
- MRI [5,18,19,20,21]

2) Pre-Processing

- Gaussian Noise
  - Median Filter [1,2,23,25,34]
  - Wiener Filter [1,2,34,39]

- Salt and Pepper Noise
  - Median Filter [1,2,23,24,25,34]
- Speckle Noise
  - Anisotropic Filter [35,40,45,49]
  - Non Local Means Filter [8,9,10,26,50]
- Rician Noise
  - Wiener Filter [1,2,39]

3) Segmentation

- Region Based method, Edge Detection, Clustering, Thresholding [6,53,54]

- Multi-Thresholding [5,29]
  - Particle Swarm Optimization algorithm [7,50,46,47]
  - Harmony Search Algorithm[28,37]
  - Differential Evolution Algorithm [36]
  - Cuckoo Search Algorithm [4,10,11,12,13,14,41,48]

4) Feature Extraction

- Discrete Wavelet Transform [16,30,38,44,42]
- Gray Level Co-occurance Matrix [3,22,30,42,43]
- Local Binary Pattern [30,32,43,50]

5) Classification

- Support Vector Machine [3,17,27,31,32]
- Random Forest [27,52]
- K – Nearest Neighbour [27,33]

4. OBJECTIVE

- The objective of brain tumor detection is to create a software model that is capable of accurately predicting and categorizing tumors based on MRI images.
- With software algorithm, brain tumor prediction will be executed very quickly with high accuracy which assist doctor to recommend treatment for patients.

5. BRAIN TUMOR DETECTION AND CLASSIFICATION

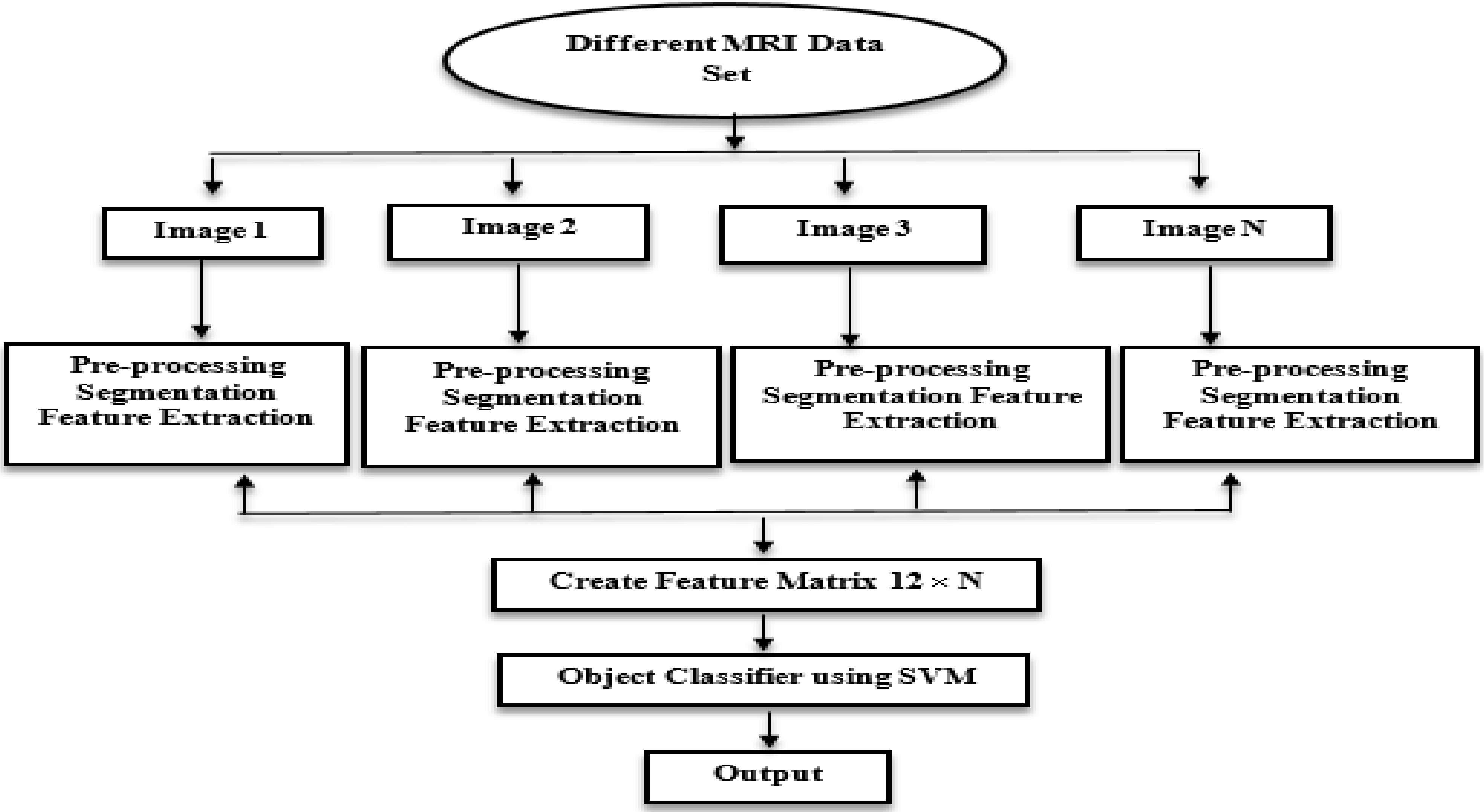

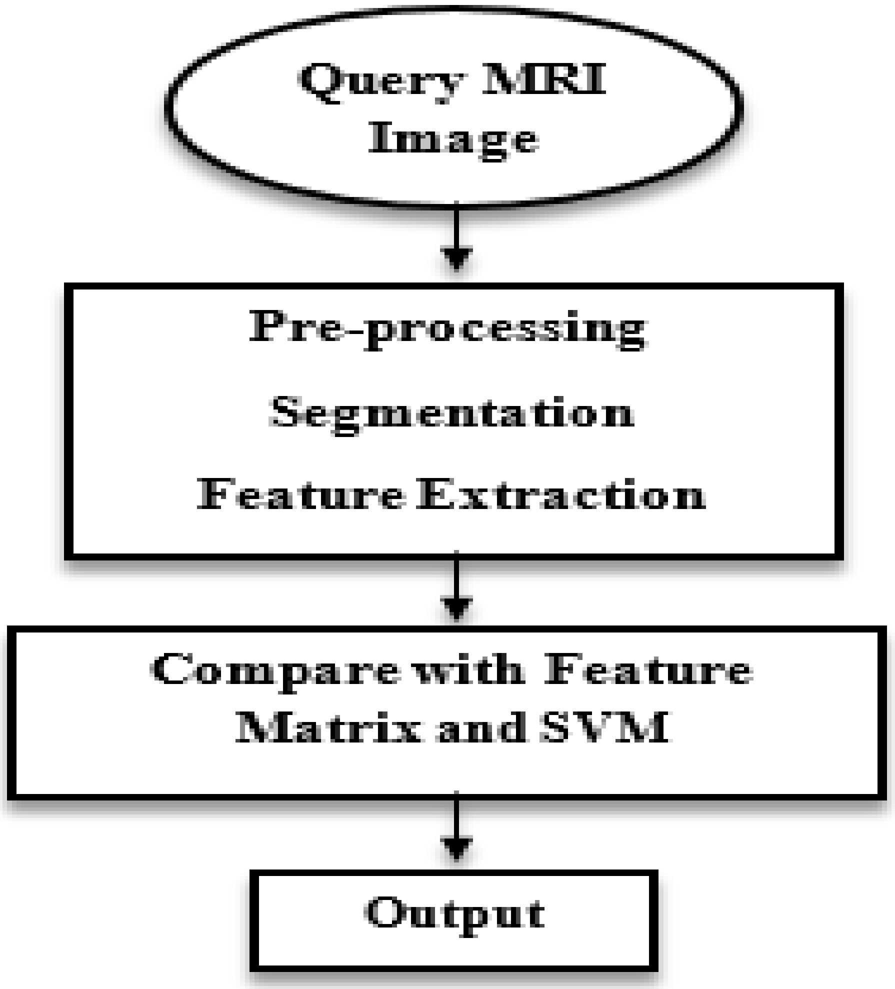
Query MRI Image
Pre-processing
Segmentation
Feature Extraction
Compare with Feature Matrix and SVM
Output

➢All the algorithms are implemented in Software and executed on the Core i3, 1.73GHz CPU with 512 GB hard disk. Image Processing toolbox, Wavelet Toolbox, etc available in Software.

1) Image Dataset:

A) kaggle dataset (www.kaggle.com)

- 600 brain images, 400 tumor images, 200 without tumor images

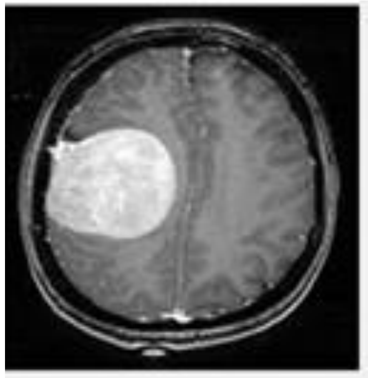

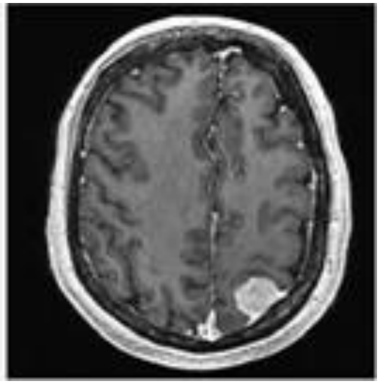

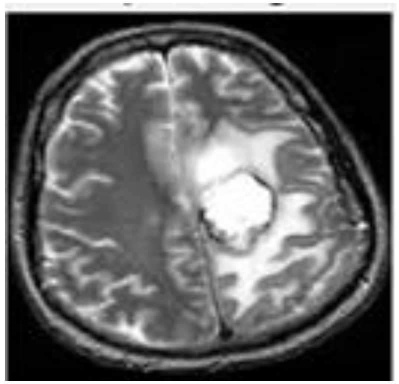

B) Sahyog Imaging Centre, SSG Hospital, Baroda Medical College, The Maharaja Sayajirao University of the Baroda, Vadodara, Gujarat, India

- 50 patients data, 30 males and 20 females patients
- 450 brain tumor images, 250 no tumor images

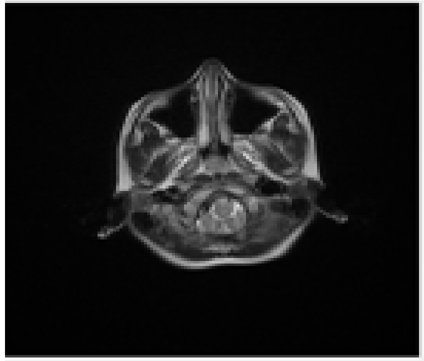

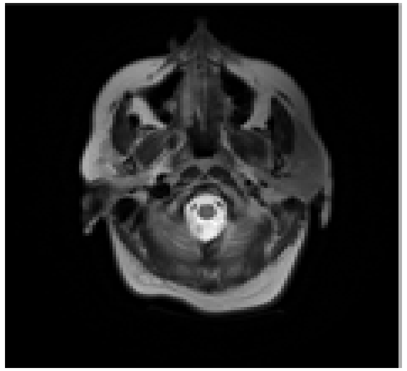

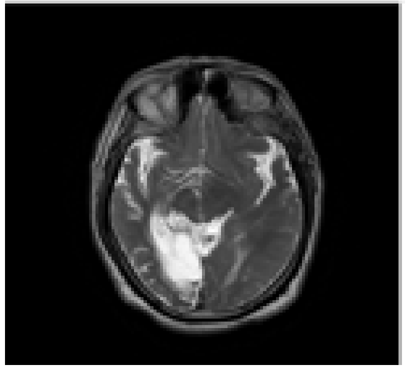

2) Pre-Processing:

❖ **Wiener Filter**

x(m, n) - degraded input image, $X(u, v)$- Discrete Fourier Transform of x(m, n),
$\hat{S}(u, v)$ - estimated value of the input image.

$$\hat{S}(u, v) = W(u, v)\, X(u, v)$$

The Wiener filter is defined as,

$$W(u, v) = \frac{H^*(u, v)}{|H(u, v)|^2 + \dfrac{P_n\ (u, v)}{P_s\ (u, v)}}$$

$H(u, v)$ - Fourier transform of the point spread function (PSF)

$P_s\ (u, v)$- Power spectrum of the signal process, generated by the application of the Fourier transform of the signal autocorrelation

$P_n\ (u, v)$ - Power spectrum of the Gaussian noise process, generated by the application of the Fourier transform of the noise autocorrelation

The inverse Fourier Transform of $\hat{S}(u, v)$, got the output(restored image).

❖Median Filter

$$Q(i, j) = \text{median}\,\{I(s, t)\}, \text{where } (s, t) \in M_{ij}\,\}$$

where Q is output image, I is the input image and M_{ij} (window/mask).

❖Anisotropic Filter

$$I_t = div(c(x, y, t).\nabla I)$$

$$c(x, y, t) = g(\|\nabla I(x, y, t)\|)$$

Where, div is the divergence operator, ∇ is the gradient, $|\nabla I|$ represents the magnitude of gradient

$$I_{i,j}^{t+1} = I_{i.j}^{t} + \lambda\,[c_N.\nabla_N I + c_S \nabla_S I + c_E \nabla_E I + c_W \nabla_W I]_{i.j}^{t}$$

The symbol ∇ indicates nearest-neighbour differences:

$$\nabla_N I_{i,j} = I_{i-1,j} - I_{i,j} \qquad \nabla_S I_{i,j} = I_{i+1,j} - I_{i,j}$$

$$\nabla_E I_{i,j} = I_{i,j+1} - I_{i,j} \qquad \nabla_W I_{i,j} = I_{i,j-1} - I_{i,j}$$

$$c_{Si.j}^{t} = g(\nabla_N I_{i.j}^{t}) \qquad c_{Ni.j}^{t} = g(\nabla_S I_{i.j}^{t})$$

$$c_{Ei.j}^{t} = g(\nabla_E I_{i.j}^{t}) \qquad c_{Wi.j}^{t} = g(\nabla_W I_{i.j}^{t})$$

For High contrast edges over low contrast ones, $g(\nabla I) = e^{\left(\frac{\|\nabla \mathrm{I}\|}{K}\right)^2}$

For wide regions over smaller ones, $g(\nabla I) = \frac{1}{1+\left(\frac{\|\nabla \mathrm{I}\|}{K}\right)^2}$, K=constant and $0 \le \lambda \le \frac{1}{4}$

❖Non Local Means Filter

In a noisy image, n = {n(i) | i ∈ I}, the projected result NL(n)(i) is quantified as a weighted mean of entire pixel of scan,

$$NL(n)(x_i) = \sum_{j \in I} q\left(x_i, x_j\right) n(x_j)$$

$q\left(x_i, x_j\right)$ indicates the weight assigned to $n(x_j)$ in attempt to recreate the pixel x_i and computed as:

$$q\left(x_i, x_j\right) = \frac{1}{Z_i}\, e^{\left(-\frac{\left(n(I)_i - n(I)_j\right)^2}{h^2}\right)}$$

I_i and I_j are the intensities of regional area foci on pixels x_i and x_j, Z_i is the standardization variable, and h is the filtration parameter

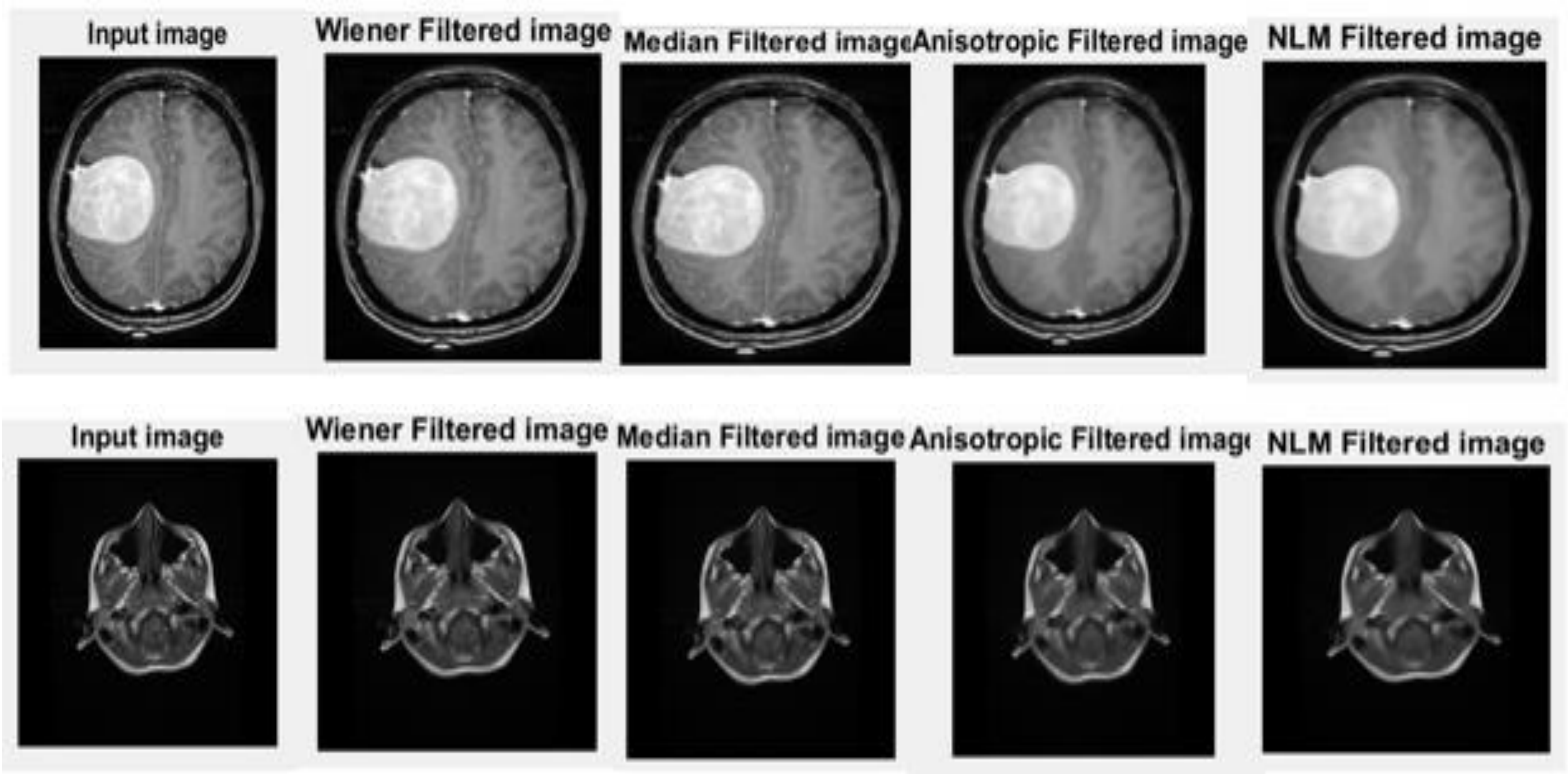

Figure-1: Implementation of different pre-processing filtering algorithms

- **Statistical parameters**

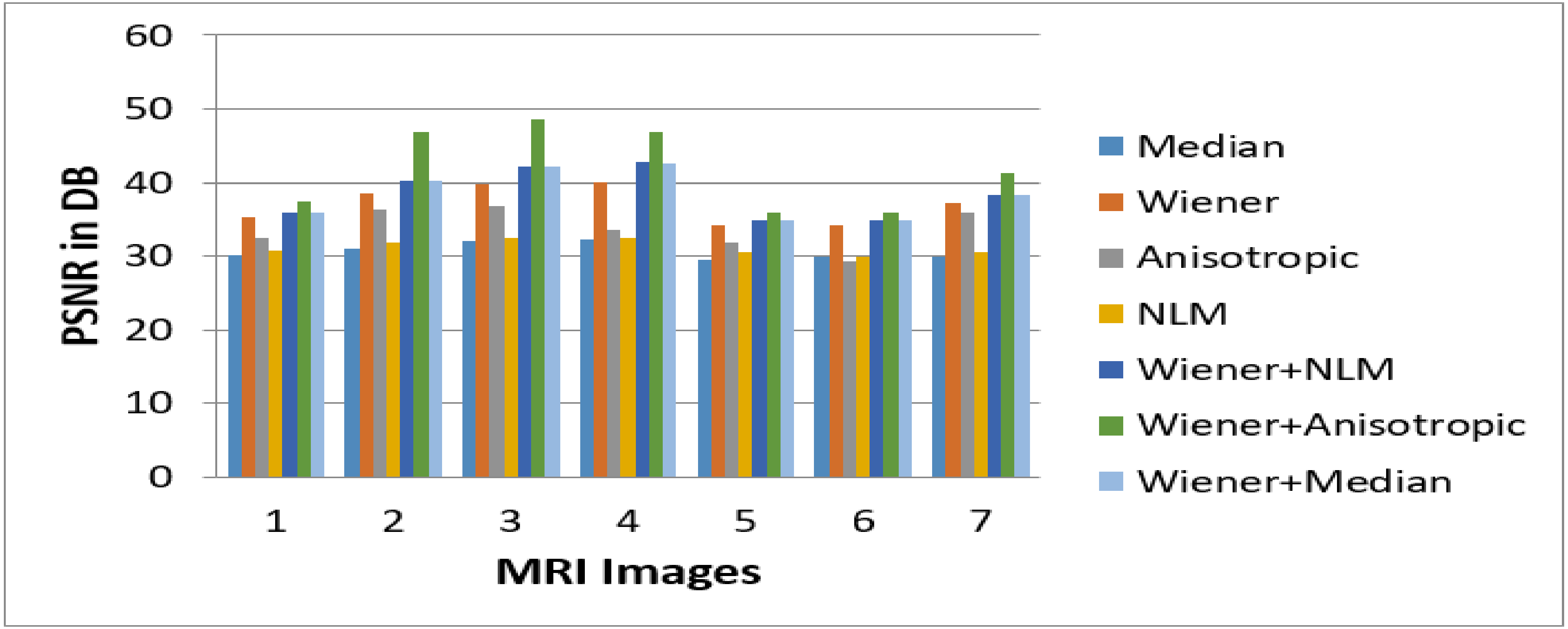

Figure-2: PSNR of the Brain Images after applying different filtering techniques

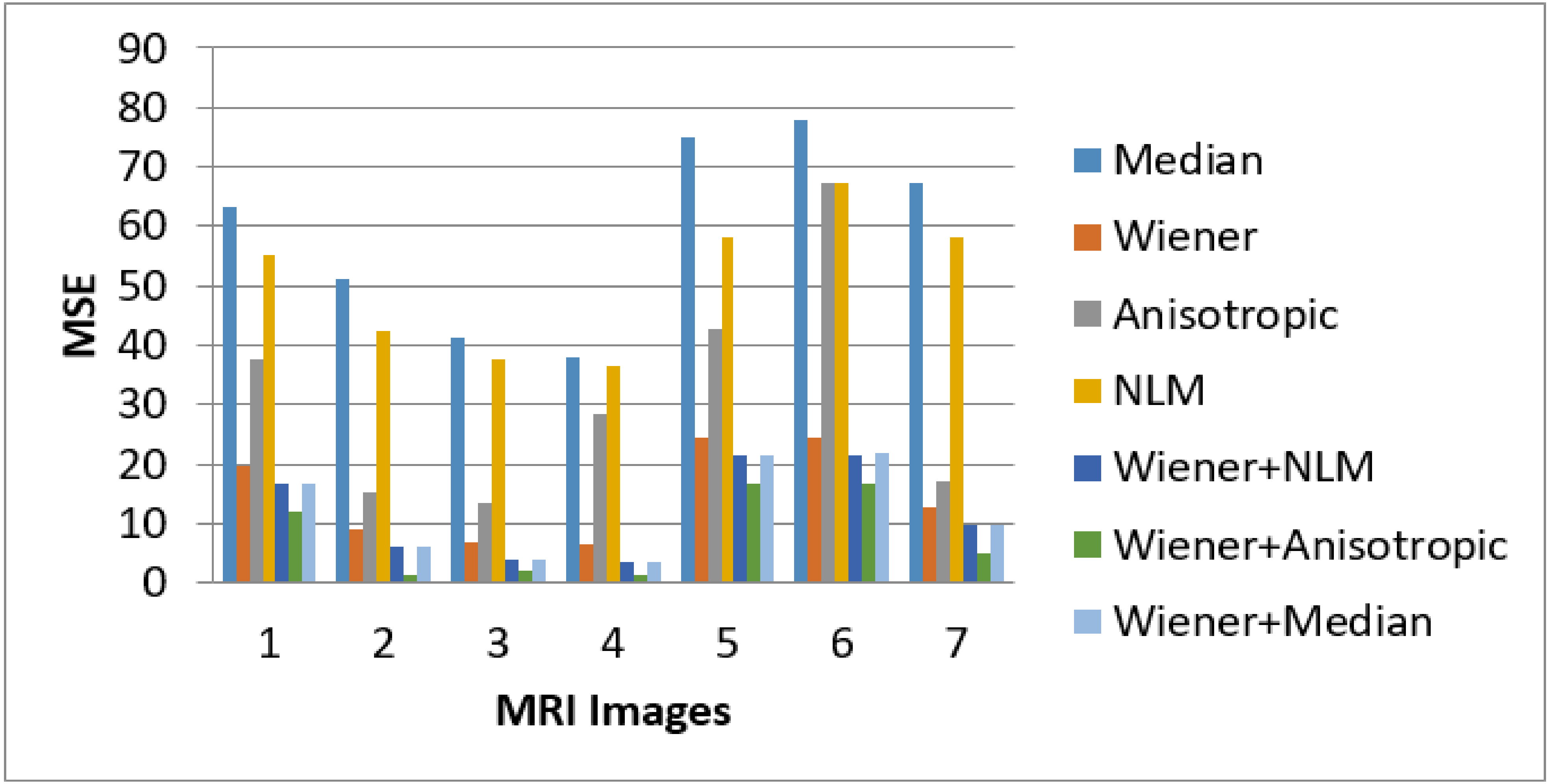

Figure-3: MSE of the Brain Images after applying different filtering techniques

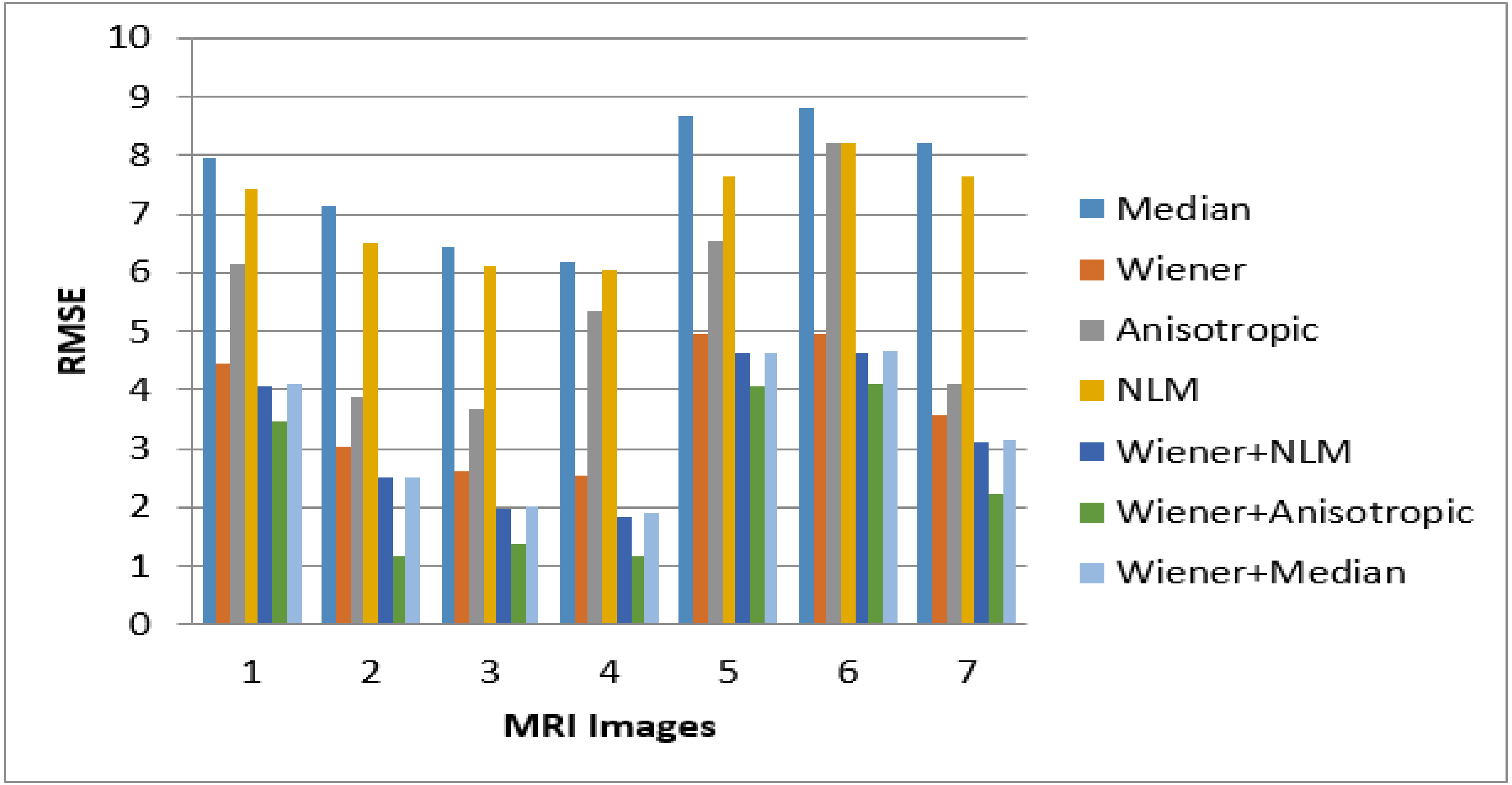

Figure-4: RMSE of the Brain Images after applying different filtering techniques

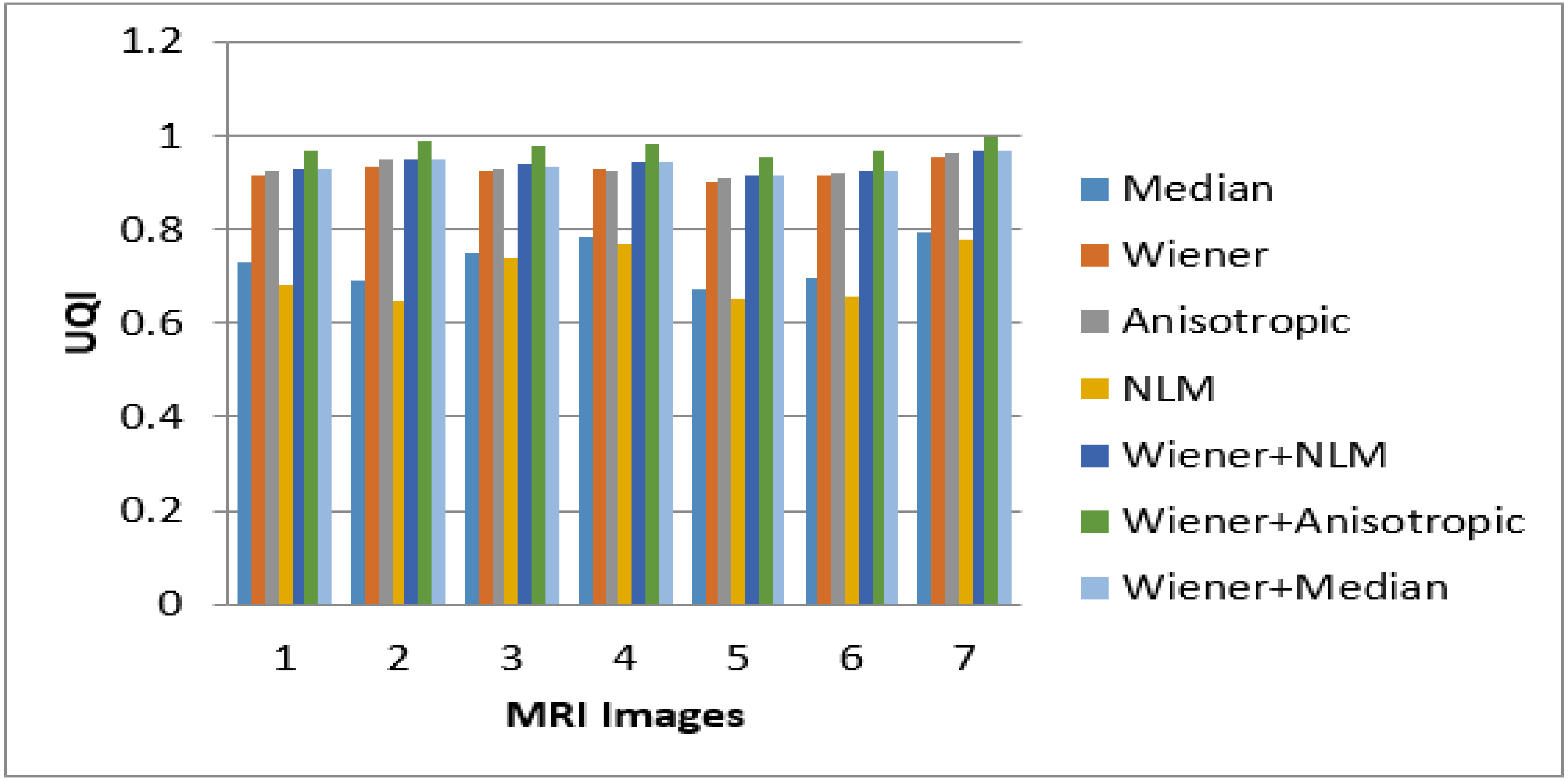

Figure-5: UQI of the Brain Images after applying different filtering techniques

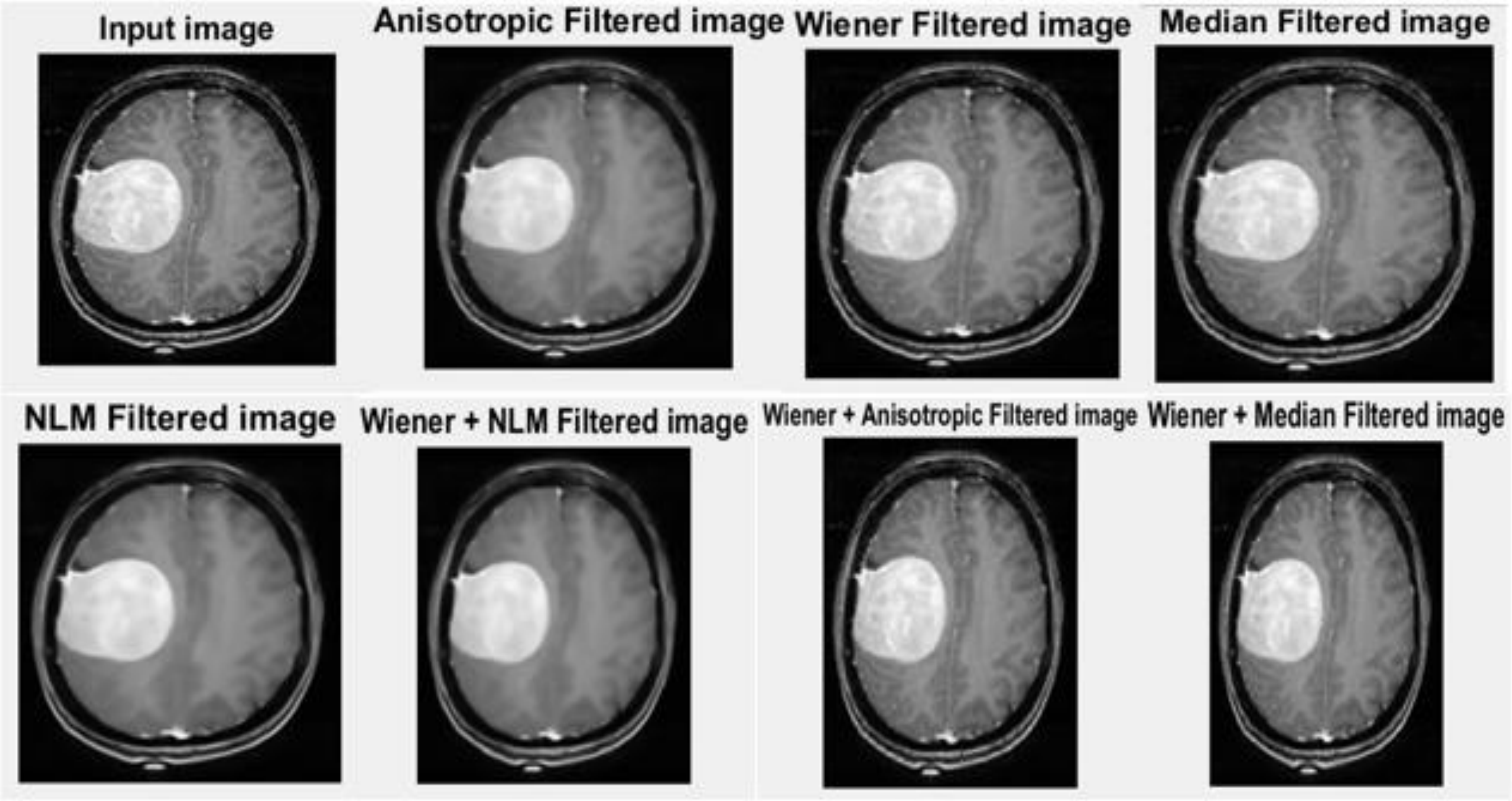

Figure-6: Implementation of different pre-processing filtering algorithms

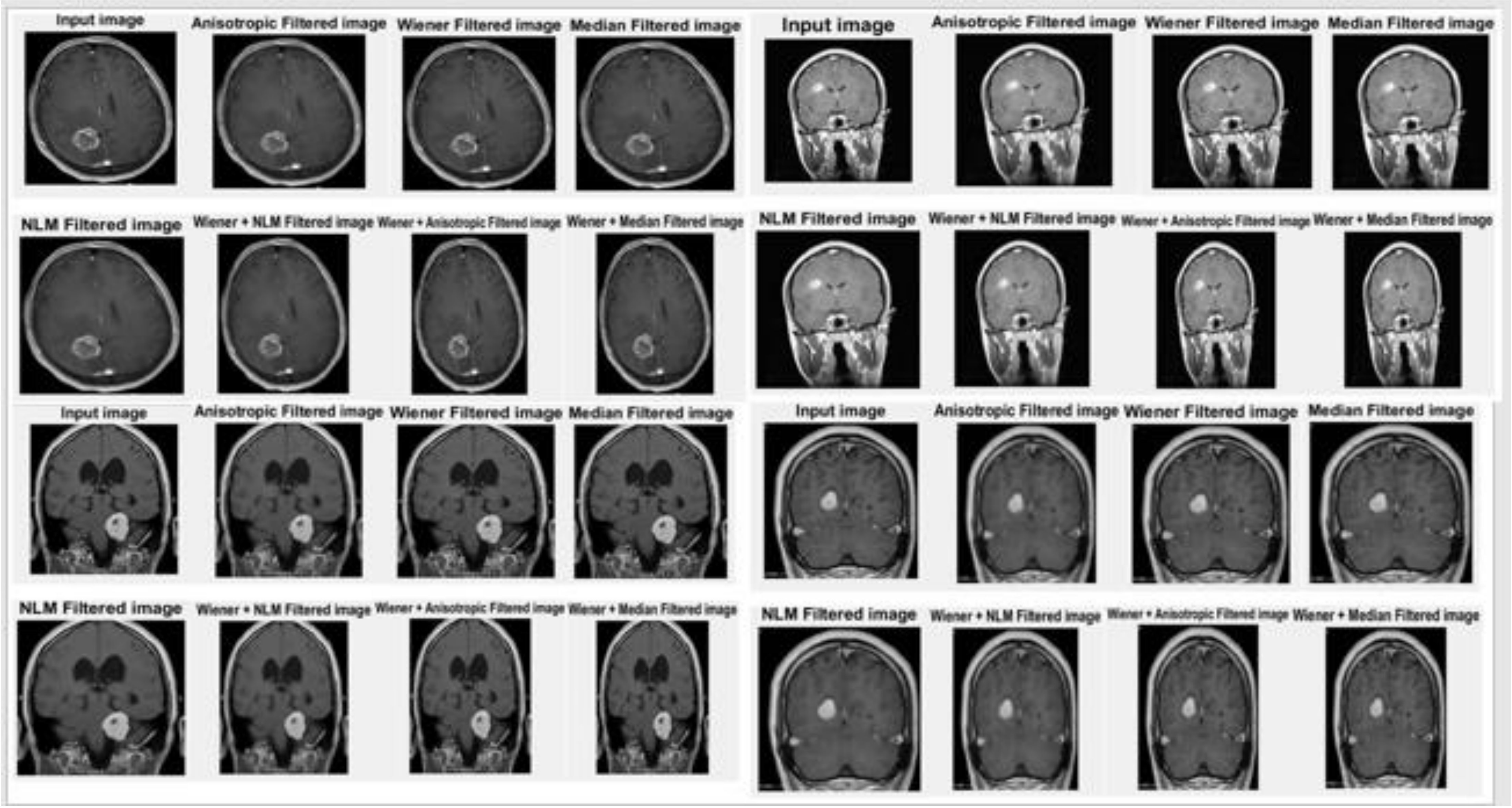

Figure-7: Implementation of different pre-processing filtering algorithms

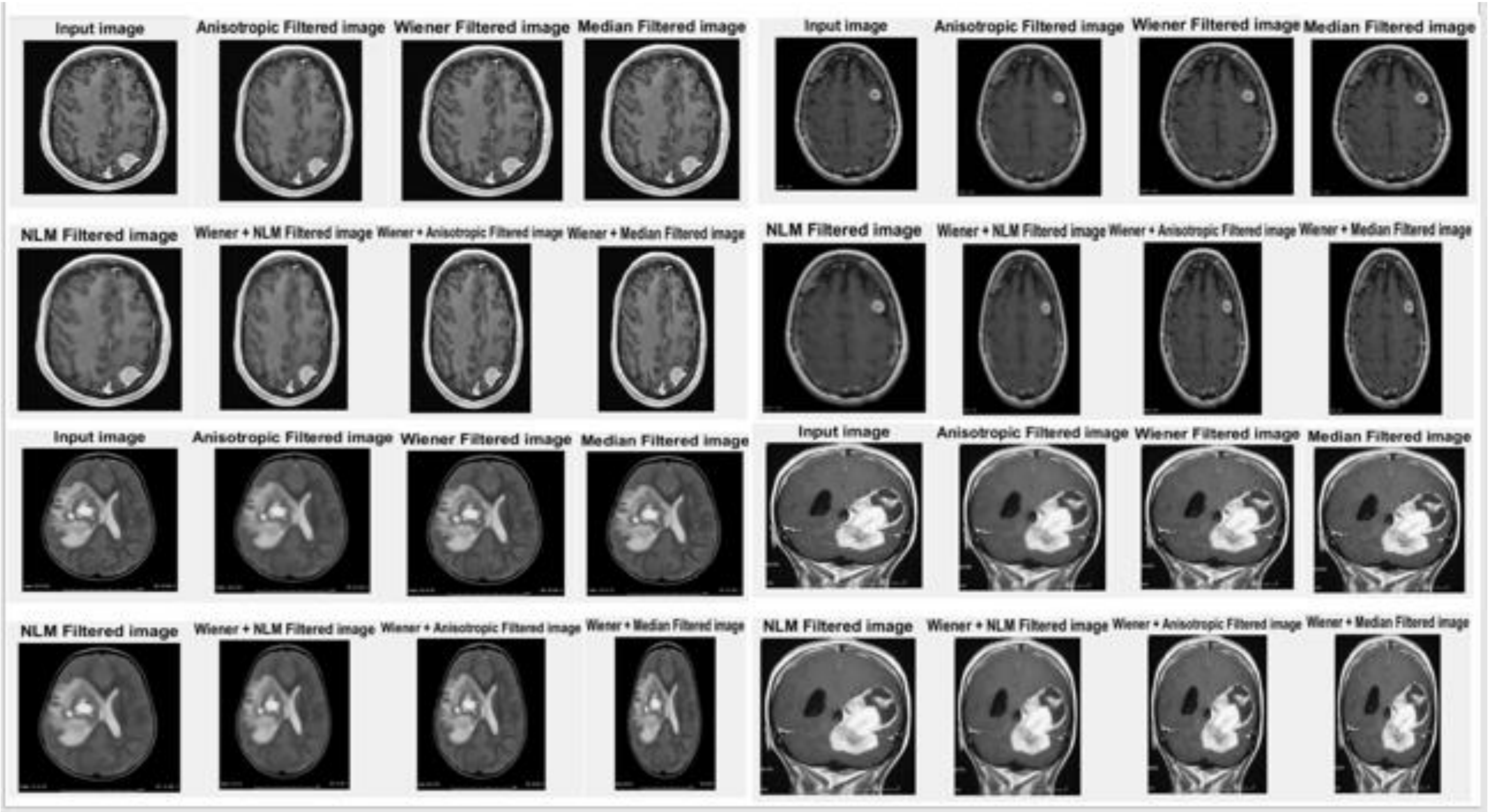

Figure-8: Implementation of different pre-processing filtering algorithms

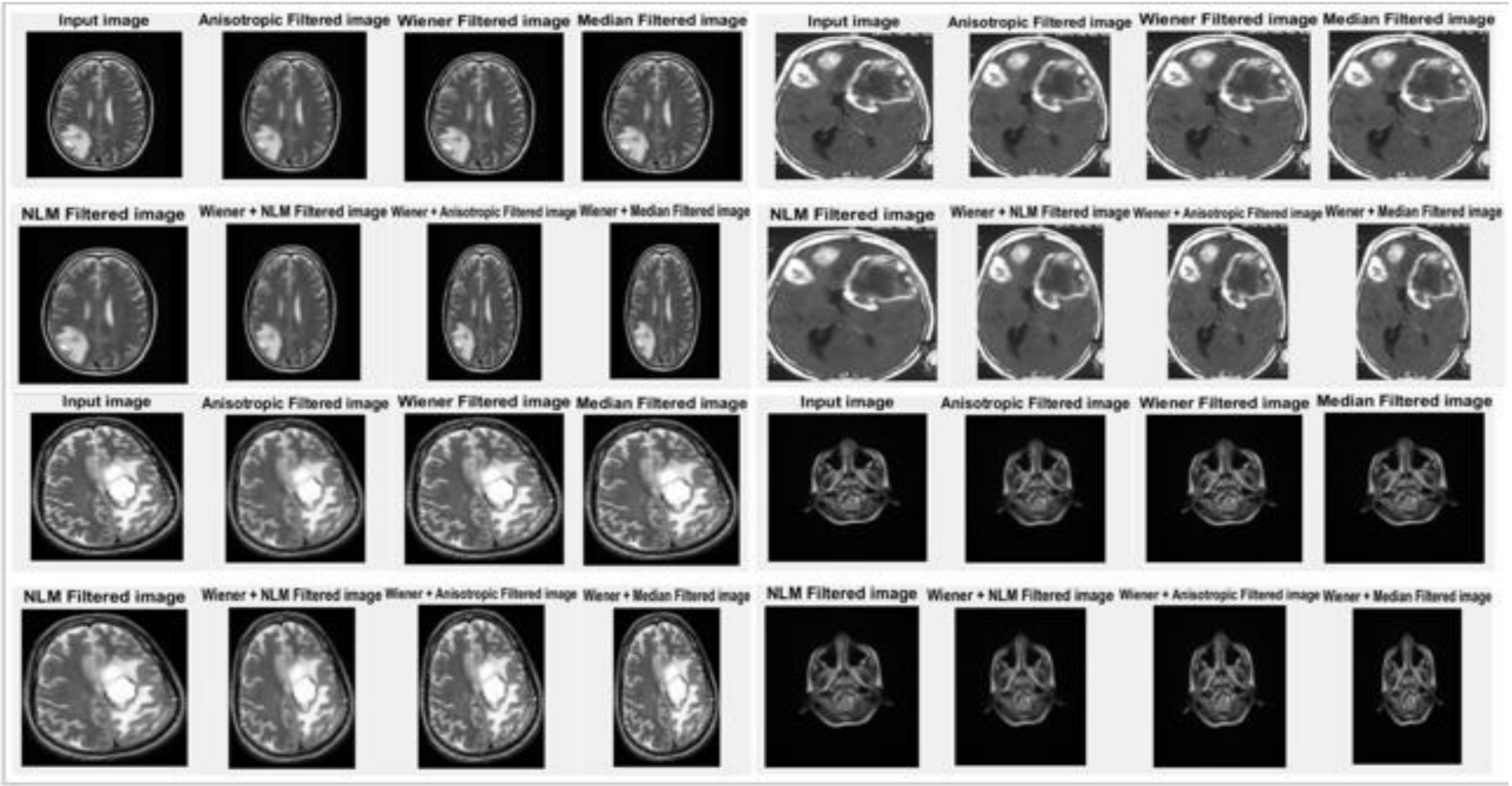

Figure-9: Implementation of different pre-processing filtering algorithms

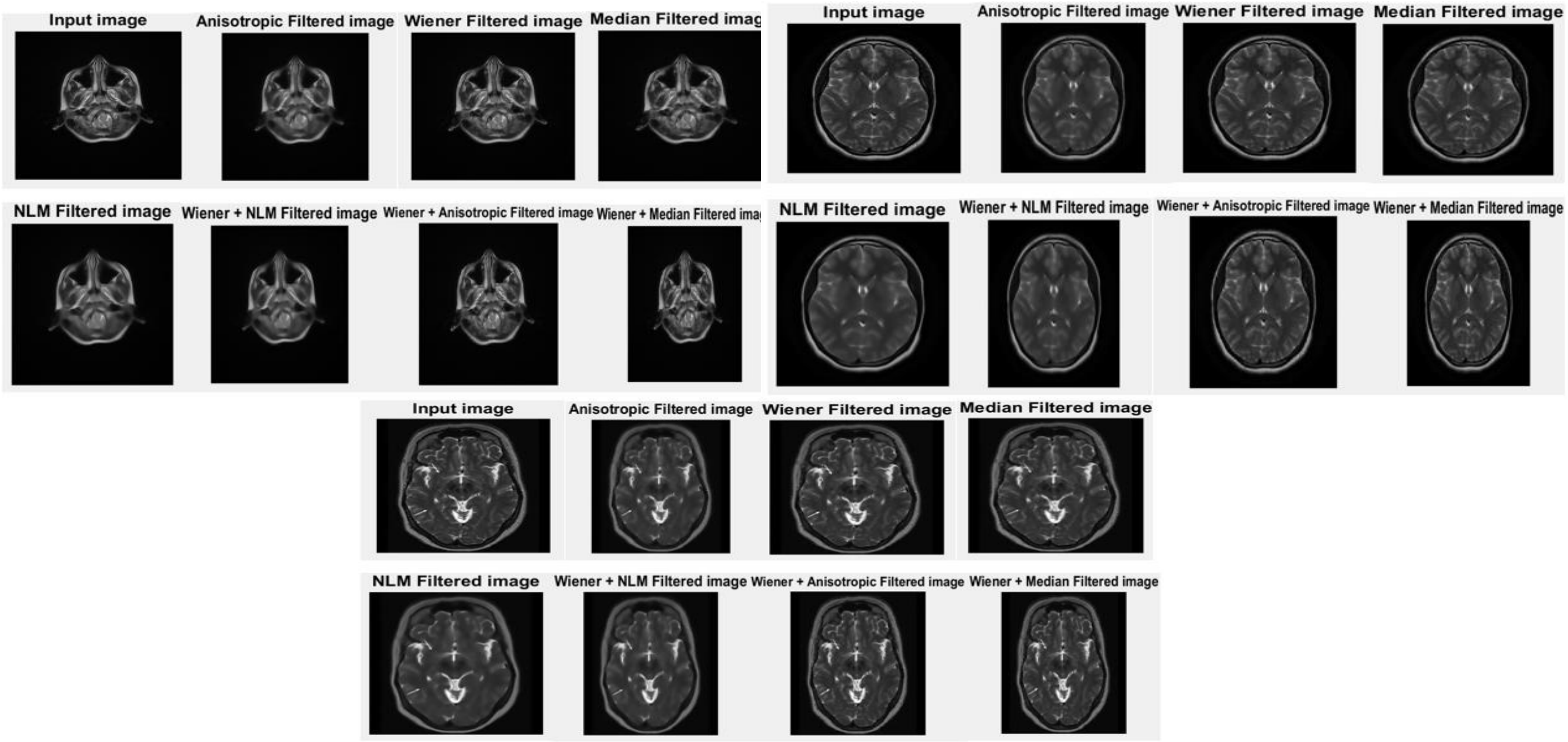

Figure-10: Implementation of different pre-processing filtering algorithms

3) Segmentation

- Bi-level Thresholding

$$TH_0 = \{J(x,y)\epsilon I: 0 \ \le J(x,y) \le th_1 - 1\}$$
$$TH_1 = \{J(x,y)\epsilon I: th_1 \ \le J(x,y) \le L - 1\}$$

- Multilevel Thresholding

$$TH_0 = \{J(x,y)\epsilon I: 0 \ \le J(x,y) \le th_1 - 1\}$$
$$TH_1 = \{J(x,y)\epsilon I: th_1 \le J(x,y) \le th_2 - 1\}$$
$$TH_i = \{J(x,y)\epsilon I: th_i \le J(x,y) \le th_{i+1} - 1\}$$
$$TH_r = \{J(x,y)\epsilon I: th_r \ \le J(x,y) \le L - 1\}$$

I - original MRI images, L - total number of distinct thresholding levels,

J(x, y) - corresponding intensity value with respect to (x, y) coordinate,

th_i = 1, 2, ⋯L

➢ Cuckoo search algorithm:

Principal of the CS algorithm [53]: :

1. Each cuckoo bird lays one egg at a time and randomly places its egg in a host bird's nest.
2. The best nests containing high-quality eggs are carried over to the next generations.
3. The number of available host nests is fixed. The host bird discovers foreign eggs with a probability p_{α}, and the range of p_{α} is from 0 to 1. The best nests are selected for further calculations.

The CS process can be summarized as follows: While generating new solution x_i^{t+1} for cuckoo i, a Lévy flight is performed:

$$x_i^{t+1} = x_i^t + \alpha_0 (x_i^t - x_{best}) \oplus Levy(\lambda)$$

α_0 - step scaling factor, x_{best} - current optimal solution

$\oplus$ - Element-wise multiplication

Levy flights are drawn from a Levy distribution, which can be defined by:

$$Levy(\lambda) \sim u = t^{-\lambda}, (1 < \lambda \leq 3)$$

Flow Chart Of The Cuckoo Search Algorithm:

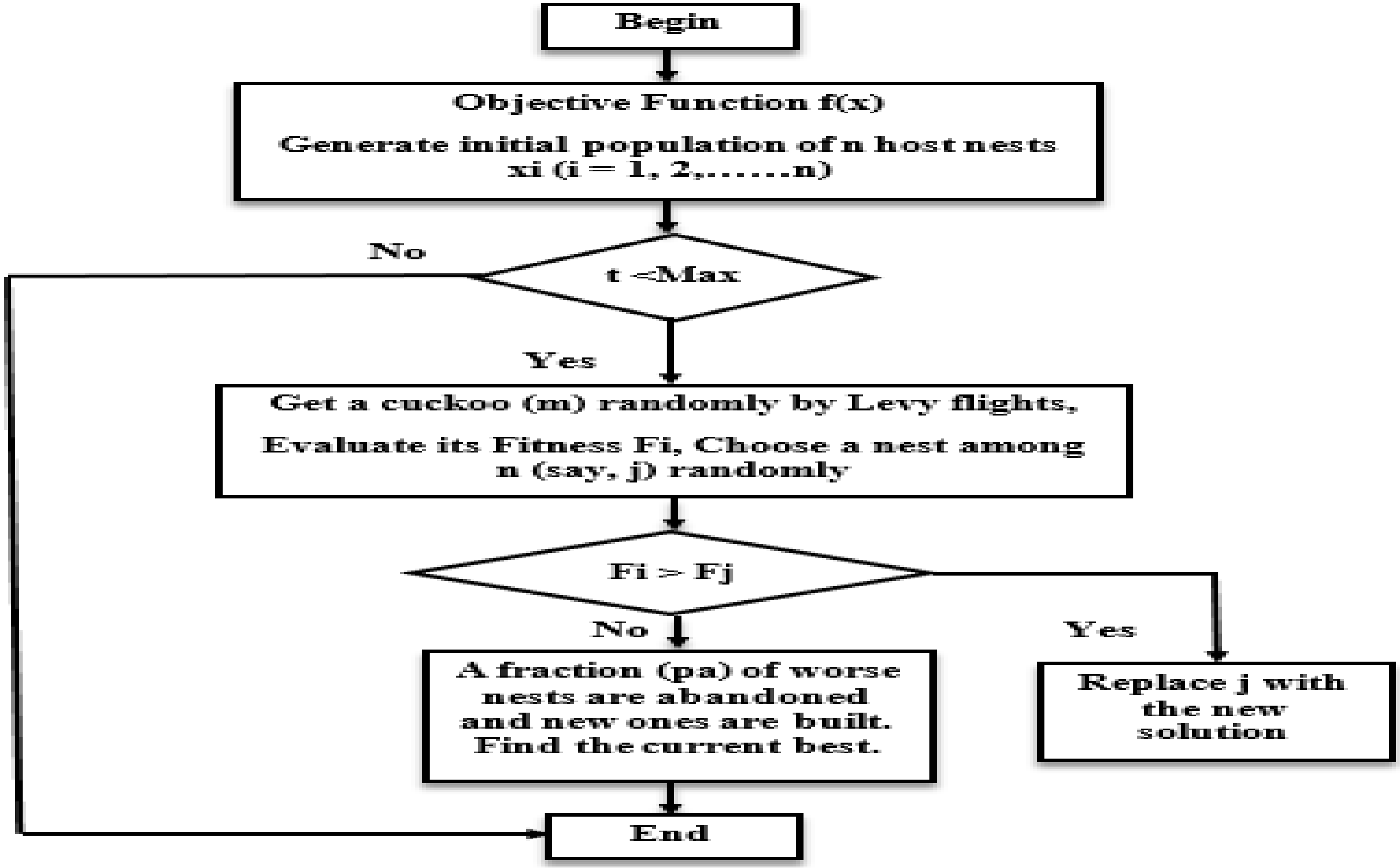

➢ Objective functions

1. Otsu’s

- To optimize between-class variance by choosing an appropriate threshold value
- p_i - probability of the pixel intensity value, i - 0 to 255
- L - total number of distinct intensity levels in the gray scale image

$$x_{best} = Arg\ max\{\sigma_B^2(t)\}$$

$$\sigma_B^2 = \sigma_0^2 + \sigma_1^2 + \sigma_2^2 + \cdots \sigma_r^2$$
$$\sigma_0^2 = \omega_0(\mu_0 - \mu_T)^2$$
$$\sigma_1^2 = \omega_1(\mu_1 - \mu_T)^2$$
$$\sigma_r^2 = \omega_r(\mu_r - \mu_T)^2$$

$$\omega_0 = \text{weight} = \frac{\sum_{i=0}^{t_1-1} p_i}{\sum_{i=0}^{L-1} p_i} \qquad \omega_1 = \text{weight} = \frac{\sum_{i=t_1}^{t_2-1} p_i}{\sum_{i=0}^{L-1} p_i}$$

$$\omega_r = \text{weight} = \frac{\sum_{i=t_r}^{L-1} p_i}{\sum_{i=0}^{L-1} p_i}$$

$$\mu_0 = \text{mean} = \frac{\sum_{i=0}^{t_1-1} i.p_i}{\sum_{i=0}^{t_1-1} p_i} \qquad \mu_1 = \text{mean} = \frac{\sum_{i=t_1}^{t_2-1} i.p_i}{\sum_{i=t_1}^{t_2-1} p_i}$$

$$\mu_r = \text{mean} = \frac{\sum_{i=t_r}^{L-1} i.p_i}{\sum_{i=t_r}^{L-1} p_i} \qquad \mu_T = \text{mean} = \frac{\sum_{i=0}^{L-1} i.p_i}{\sum_{i=0}^{L-1} p_i}$$

2. Kapur Entropy

$$x_{best} = Arg\ max\{H_T(t)\}$$

$$H_T = H_0 + H_1 + H_2 \ldots + H_r$$

$$H_0 = -\sum_{i=0}^{t_1-1} \frac{p_i}{w(0)} ln \frac{p_i}{w(0)}$$

$$H_1 = -\sum_{i=t_1}^{t_2-1} \frac{p_i}{w(1)} ln \frac{p_i}{w(1)}$$

$$H_2 = -\sum_{i=t_2}^{t_3-1} \frac{p_i}{w(1)} ln \frac{p_i}{w(2)}$$

$$H_r = -\sum_{i=t_r}^{L-1} \frac{p_i}{w(r)} ln \frac{p_i}{w(r)}$$

$$w(0) = \sum_{i=0}^{t_1-1} p_i$$

$$w(1) = \sum_{i=t_1}^{t_2-1} p_i$$

$$w(2) = \sum_{i=t_2}^{t_3-1} p_i$$

$$w(r) = \sum_{i=t_m}^{L-1} p_i$$

3. Tsallis Entropy

$$x_{best} = Arg\ max\{S_T(t)\}$$

$$S_T = S_0 + S_1 + S_2 \ldots + S_r + (1 - q).(S_0.S_1.S_2 \ldots .S_r)$$

$$S_0 = \frac{1 - \sum_{i=0}^{t_1 - 1}\left(\frac{p_i}{w(0)}\right)^q}{q-1} \qquad w(0) = \sum_{i=0}^{t_1 - 1} p_i$$

$$S_1 = \frac{1 - \sum_{i=t_1}^{t_2 - 1}\left(\frac{p_i}{w(1)}\right)^q}{q-1} \qquad w(1) = \sum_{i=t_1}^{t_2 - 1} p_i$$

$$S_r = \frac{1 - \sum_{i=t_r}^{L - 1}\left(\frac{p_i}{w(r)}\right)^q}{q-1} \qquad w(r) = \sum_{i=t_m}^{L - 1} p_i$$

4. Combined Otsu with Tsallis Entropy

$$x_{best} = Arg\ max\{\mu(t)\}$$

$$\mu(t) = S_T - (\sigma_B^2)^{1-q}$$

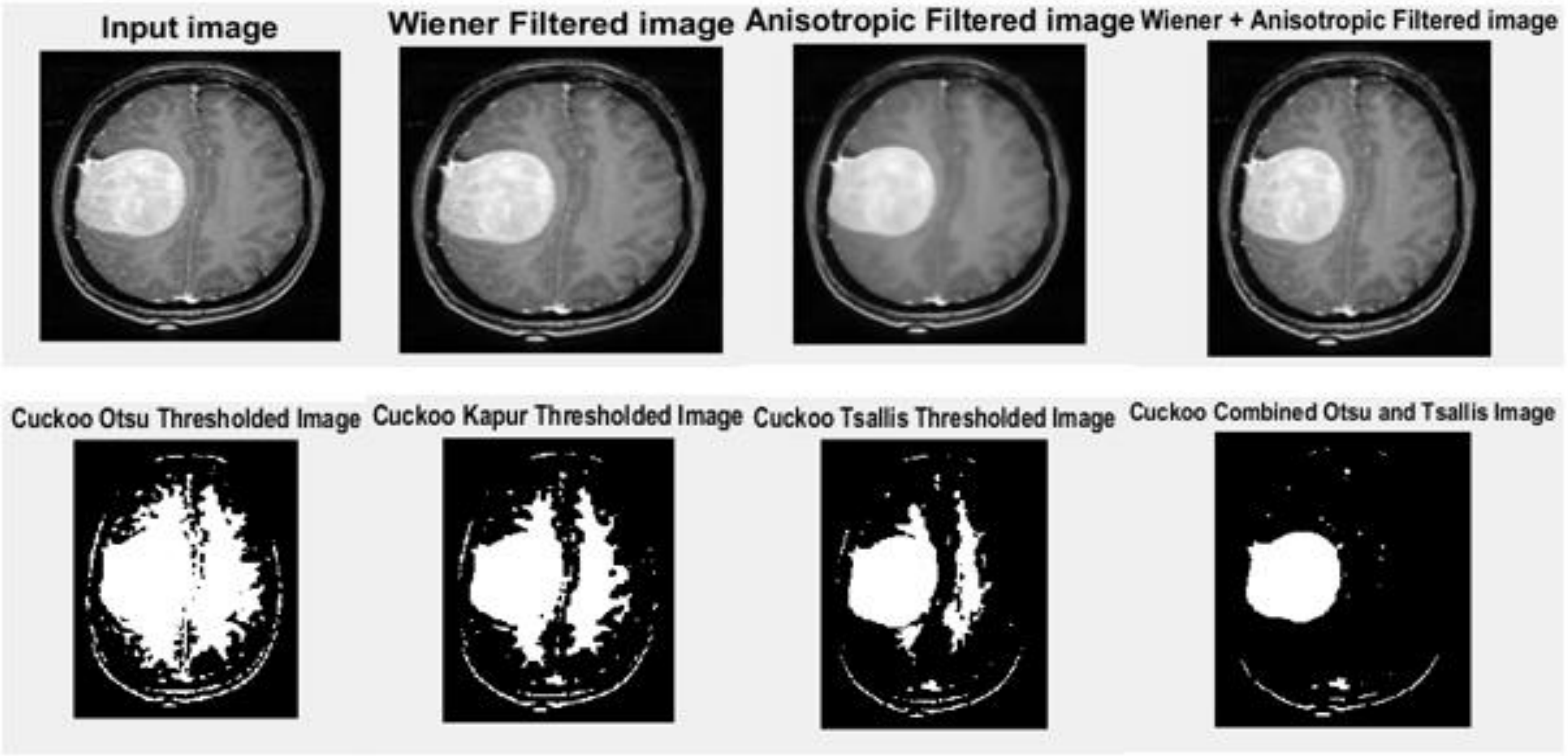

Figure-11: Implementation of different segmentation techniques

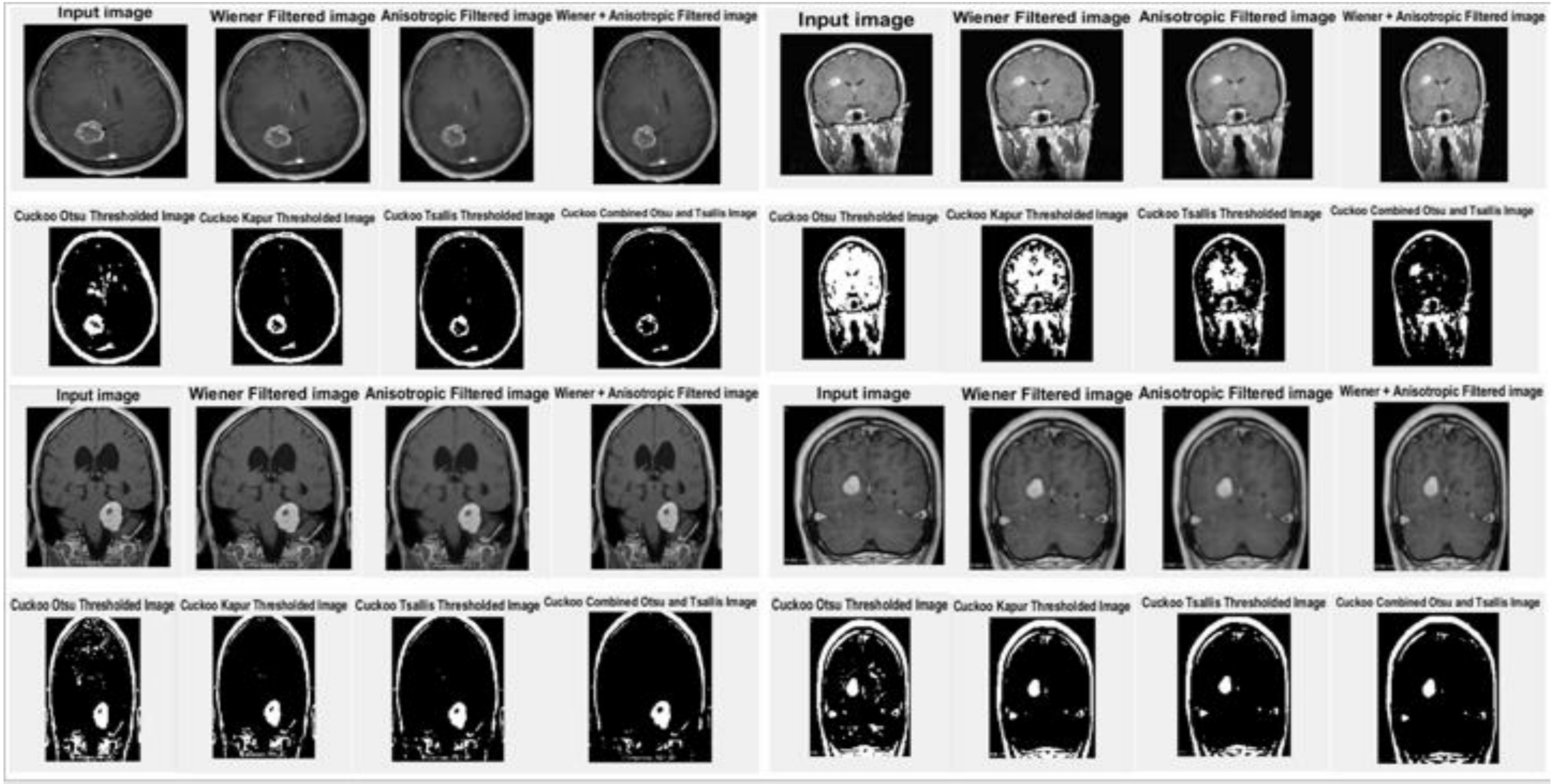

Figure-12: Implementation of different segmentation techniques

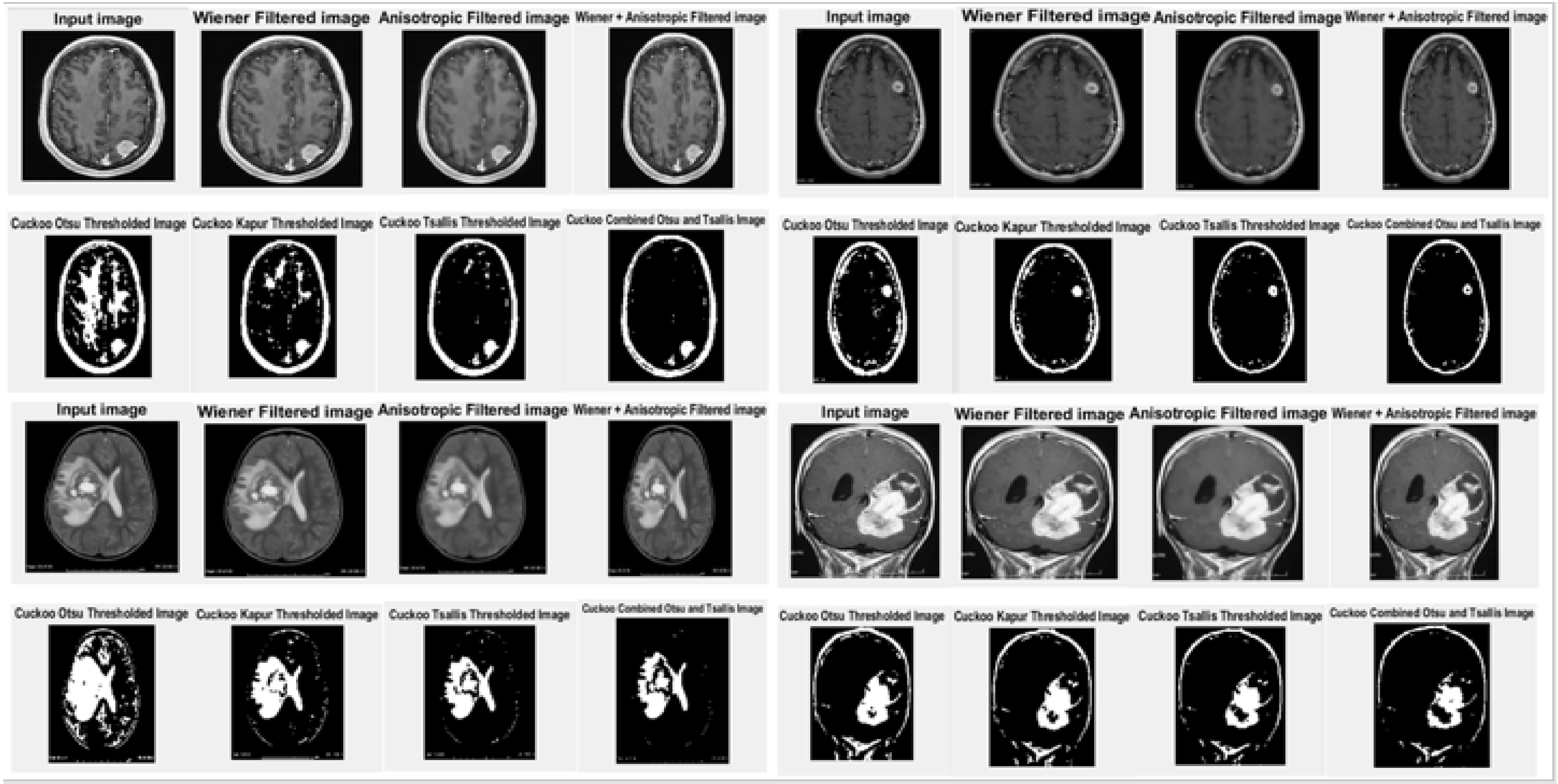

Figure-13: Implementation of different segmentation techniques

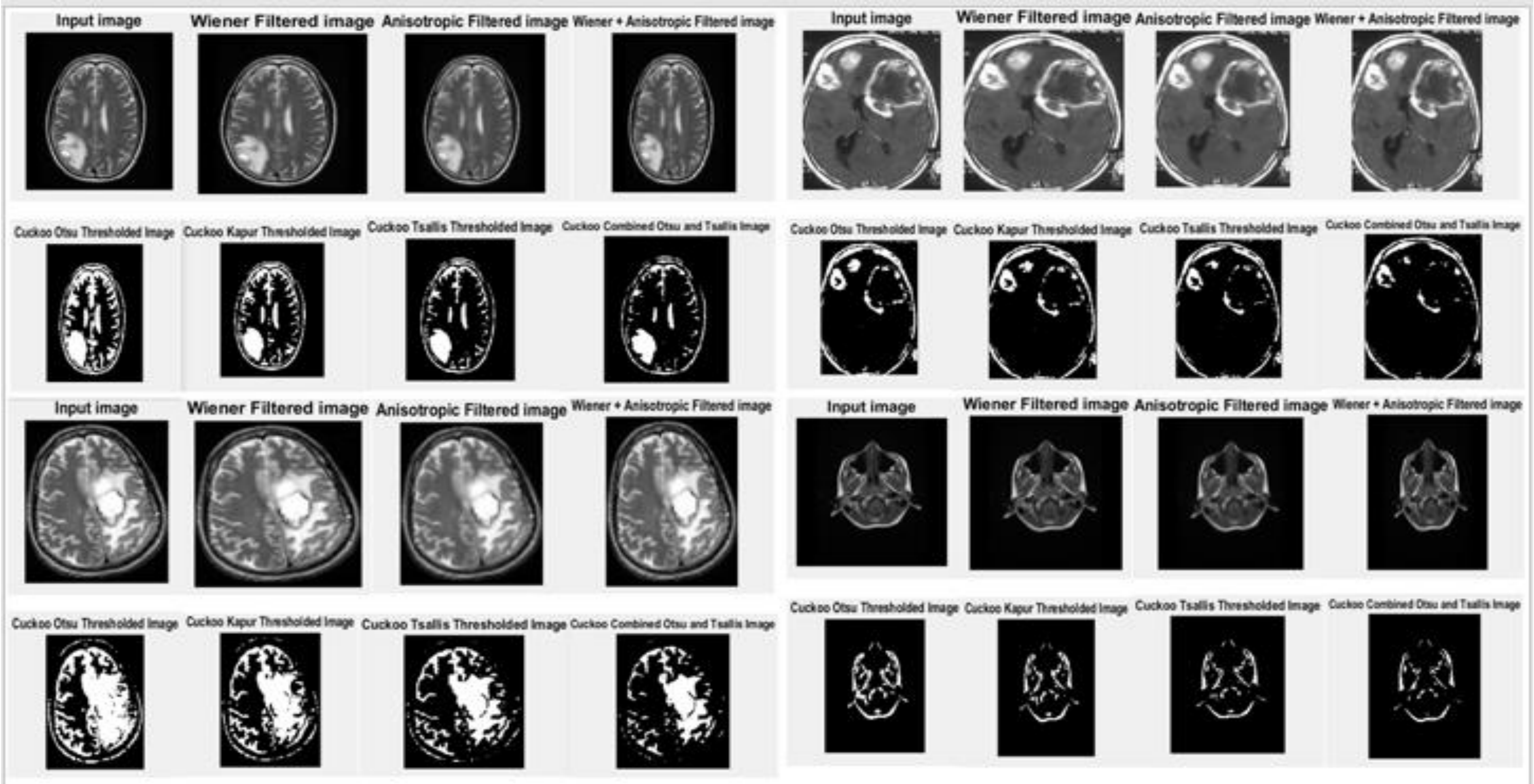

Figure-14: Implementation of different segmentation techniques

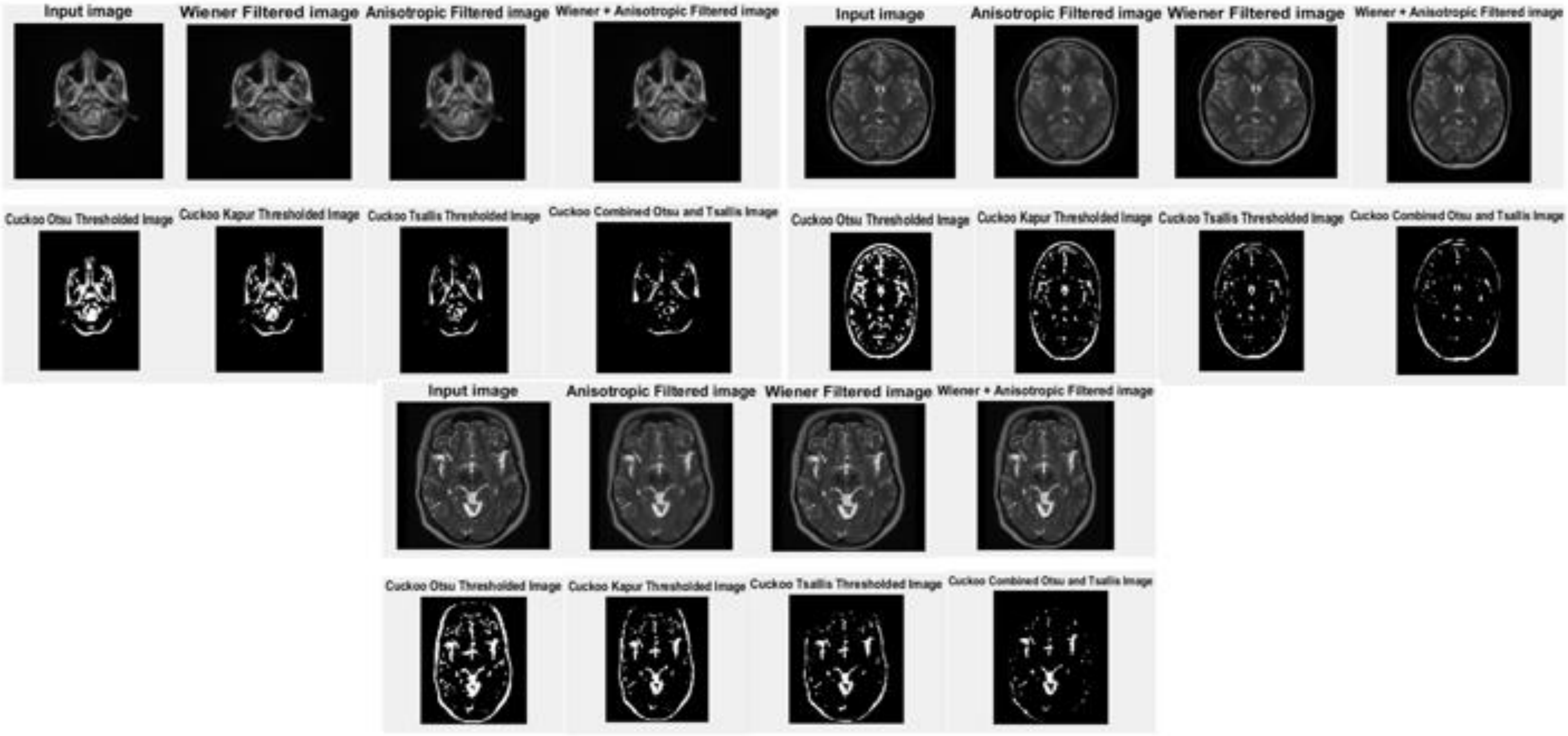

Figure-15: Implementation of different segmentation techniques

4) Feature Extraction

DWT works by applying a series of filters to the input signal or image, which separate it into low-frequency and high-frequency components. These components can then be further decomposed into sub-bands, creating a tree-like structure known as a wavelet decomposition.

The coefficients can be computed using filter banks, where the LL coefficients represent the low-frequency approximation and the remaining coefficients represent the high-frequency details in different directions.

- x(n) - input signal or image,
- h(n) - low-pass filter coefficients
- g(n) - high-pass filter coefficients

The DWT equations for obtaining the LL, LH, HL, and HH coefficients can be written as follows:

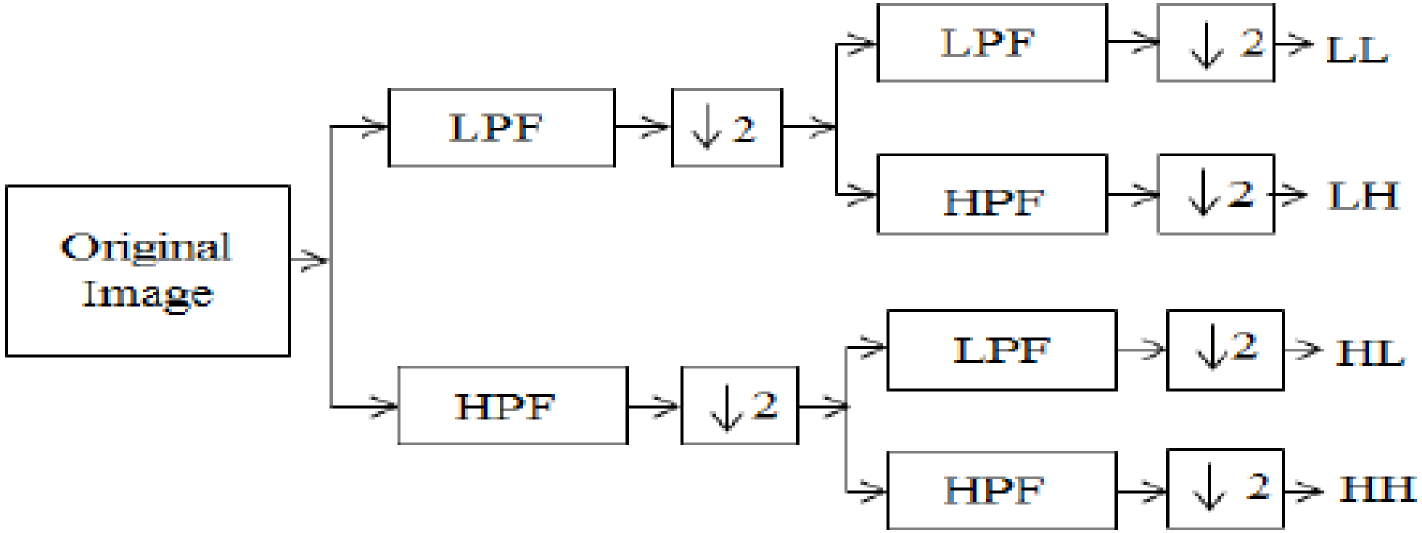

$$LL(n) = x * h * h \ (downsampling\ by\ 2)$$
$$LH(n) = x * h * g \ (downsampling\ by\ 2)$$
$$HL(n) = x * g * h \ (downsampling\ by\ 2)$$
$$HH(n) = x * g * g \ (downsampling\ by\ 2)$$

- downsampling by 2 - reduces the size of the coefficients by half, * - convolution

- **Statistical Parameters**

Image	Contrast	Correlation	Energy	Homogeneity	Mean	Standard Deviation
Image 1	0.2539	0.1014	0.7610	0.9329	0.0017	0.0892
Image 2	0.2258	0.1529	0.7689	0.9364	0.0017	0.0892
Image 3	0.2152	0.1143	0.7526	0.9326	0.0048	0.0896
Image 4	0.3167	0.1297	0.7949	0.9395	0.0075	0.0899
Image 5	0.243	0.0943	0.7488	0.9300	0.0050	0.0897
Image 6	0.23	0.0871	0.7513	0.9301	0.0046	0.0895
Image 7	0.2364	0.1479	0.7429	0.9287	0.0046	0.0895

Figure-16: Statistical parameters (1 to 6) for different brain images

Image	Entropy	RMS	Variance	Kurtosis	Skewness	Inverse Different Moment
Image 1	2.9641	0.0898	0.0081	7.8474	0.5534	0.1548
Image 2	3.0447	0.0897	0.0082	7.2954	0.3964	0.6042
Image 3	3.7365	0.0868	0.0081	5.8455	0.4031	1.5651
Image 4	3.1611	0.0892	0.0080	13.499	1.3523	0.8302
Image 5	3.614	0.0892	0.0081	6.052	0.5247	1.1661
Image 6	3.7295	0.0848	0.0082	5.6958	0.3829	0.5801
Image 7	3.5494	0.0886	0.0081	6.573	0.6144	0.3837

Figure-17: Statistical parameters (7 to 12) for different brain images

5) Feature Classification

Support Vector Machine is used for classification. The basic idea behind SVM is to transform the input data into a higher-dimensional space, where it becomes easier to find a decision boundary that separates the different classes. This decision boundary is defined by a hyperplane that maximizes the margin between the two closest points from different classes. The points that lie on the margin are called support vectors, hence the name Support Vector Machines.

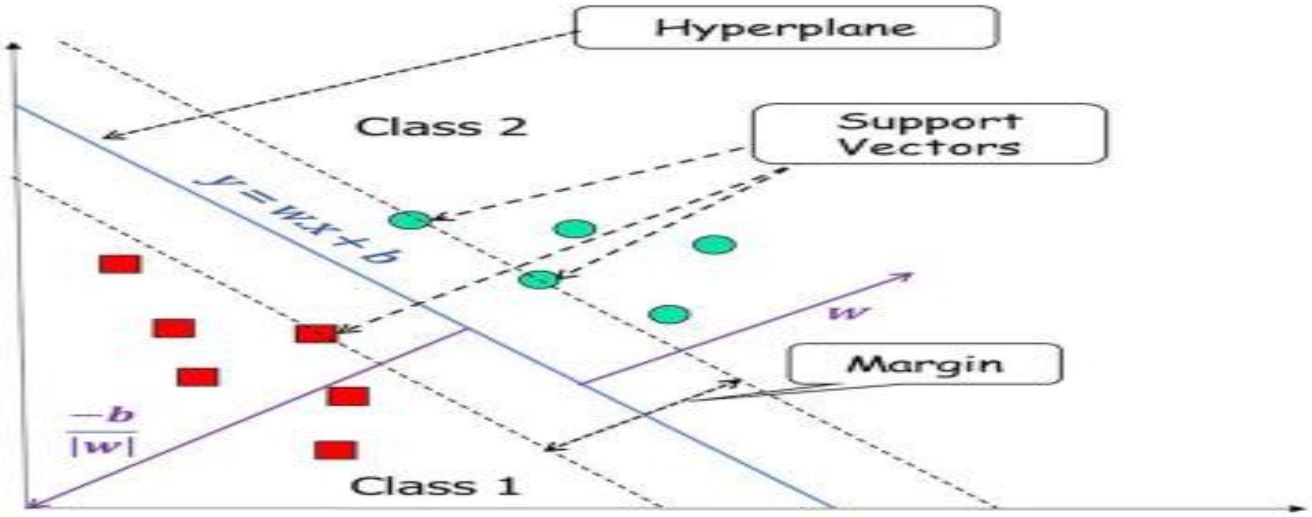

- 2×2 Confusion Matrix

Total Brain Images		Predicted	
		With Brain Tumor	Without Brain Tumor
Actual	With Brain Tumor	TP	FN
	Without Brain Tumor	FP	TN

- 2×2 Confusion Matrix with Combined Wiener and Anisotropic Filter using Cuckoo Search Algorithm with Otsu as an Objective function

Total Brain Images – 170 With Brain Tumor Images – 110 Without Brain Tumor Images - 60		Predicted	
		With Brain Tumor	Without Brain Tumor
Actual	With Brain Tumor	100	10
	Without Brain Tumor	07	53

- 2×2 Confusion Matrix with Combined Wiener and Anisotropic Filter using Cuckoo Search Algorithm with Kapur Entropy as an Objective function

Total Brain Images – 170 With Brain Tumor Images – 110 Without Brain Tumor Images - 60		Predicted	
		With Brain Tumor	Without Brain Tumor
Actual	With Brain Tumor	103	07
	Without Brain Tumor	05	55

- 2×2 Confusion Matrix with Combined Wiener and Anisotropic Filter using Cuckoo Search Algorithm with Tsallis Entropy as an Objective function

Total Brain Images – 170 With Brain Tumor Images – 110 Without Brain Tumor Images - 60		Predicted	
		With Brain Tumor	Without Brain Tumor
Actual	With Brain Tumor	106	04
	Without Brain Tumor	04	56

- 2×2 Confusion Matrix with Combined Wiener and Anisotropic Filter using Cuckoo Search Algorithm with Combined Otsu and Tsallis Entropy as an Objective function

Total Brain Images – 170 With Brain Tumor Images – 110 Without Brain Tumor Images - 60		Predicted	
		With Brain Tumor	**Without Brain Tumor**
Actual	**With Brain Tumor**	**108**	**02**
	Without Brain Tumor	**03**	**57**

- Performance evaluation statistical parameters

$$Negative\ Predictive\ Value\ (NPV) = \frac{TN}{TN+FN} \qquad Specificity\ (S_p) = \frac{TN}{FP+TN}$$

$$Positive\ Predictive\ Value\ (PPV) = \frac{TP}{TP+FP} \qquad Sensitivity\ (S_e) = \frac{TP}{TP+FN}$$

$$Accuracy\ (Acc) = \frac{TP + TN}{TP + FN + TN + FP}$$

Parameters	Combined Wiener and Anisotropic Filter using CSA with Otsu as an Objective function	Combined Wiener and Anisotropic Filter using CSA with Kapur Entropy as an Objective function	Combined Wiener and Anisotropic Filter using CSA with Tsallis Entropy as an Objective function	Combined Wiener and Anisotropic Filter using CSA with Combined Otsu and Tsallis Entropy as an Objective function
Se	0.909	0.936	0.9636	0.981
Sp	0.8833	0.9166	0.9333	0.9500
PPV	0.9345	0.9537	0.9636	0.9729
NPV	0.8412	0.8870	0.9333	0.9661
Acc	0.900	0.929	0.952	0.970

Figure-18: Performance evaluation statistical parameters for brain tumor classification using 2×2 Confusion Matrix

- 3×3 Confusion matrix

Total Brain Images – 340 With Brain Tumor Images – 220 Without Brain Tumor Images - 120		Predicted		
		With Benign Brain Tumor	With Malignant Brain Tumor	Without Brain Tumor
Actual	With Benign Brain Tumor	A	B	C
	With Malignant Brain Tumor	D	E	F
	Without Brain Tumor	G	H	I

- 3×3 Confusion Matrix with Combined Wiener and Anisotropic Filter using Cuckoo Search Algorithm with Otsu as an Objective function

Total Brain Images – 340 With Brain Tumor Images – 220 Without Brain Tumor Images - 120		Predicted		
		With Benign Brain Tumor	With Malignant Brain Tumor	Without Brain Tumor
Actual	With Benign Brain Tumor	120	06	04
	With Malignant Brain Tumor	06	80	04
	Without Brain Tumor	08	06	106

- 3×3 Confusion Matrix with Combined Wiener and Anisotropic Filter using Cuckoo Search Algorithm with Kapur Entropy as an Objective function

Total Brain Images – 340 With Brain Tumor Images – 220 Without Brain Tumor Images - 120		Predicted		
		With Benign Brain Tumor	With Malignant Brain Tumor	Without Brain Tumor
Actual	With Benign Brain Tumor	124	03	03
	With Malignant Brain Tumor	04	82	04
	Without Brain Tumor	06	04	110

- 3×3 Confusion Matrix with Combined Wiener and Anisotropic Filter using Cuckoo Search Algorithm with Tsallis Entropy as an Objective function

Total Brain Images – 340 With Brain Tumor Images – 220 Without Brain Tumor Images - 120		Predicted		
		With Benign Brain Tumor	With Malignant Brain Tumor	Without Brain Tumor
Actual	With Benign Brain Tumor	127	01	02
	With Malignant Brain Tumor	03	85	02
	Without Brain Tumor	05	03	112

- 3×3 Confusion Matrix with Combined Wiener and Anisotropic Filter using Cuckoo Search Algorithm with Combined Otsu and Tsallis Entropy as an Objective function

Total Brain Images – 340 With Brain Tumor Images – 220 Without Brain Tumor Images - 120		Predicted		
		With Benign Brain Tumor	With Malignant Brain Tumor	Without Brain Tumor
Actual	With Benign Brain Tumor	128	01	01
	With Malignant Brain Tumor	01	88	01
	Without Brain Tumor	04	02	114

- TP, FP, TN, FN

A	B	C
D	E	F
G	H	I

	Benign Tumor	Maligant Tumor	Without Tumor
TP	A	E	I
FP	D+G	B+H	C+F
TN	E+F+H+I	A+C+G+I	A+B+D+E
FN	B+C	D+F	G+H

	Combined Wiener and Anisotropic Filter using CSA with Otsu as an Objective function	Combined Wiener and Anisotropic Filter using CSA with Kapur Entropy as an Objective function	Combined Wiener and Anisotropic Filter using CSA with Tsallis Entropy as an Objective function	Combined Wiener and Anisotropic Filter using CSA with Combined Otsu and Tsallis Entropy as an Objective function
TP(Benign)	120	124	127	128
TP(Malignant)	80	82	85	88
TP(Without Tumor)	106	110	112	114
FP(Benign)	14	10	08	05
FP(Malignant)	12	07	04	03
FP(Without Tumor)	08	07	04	02
TN(Benign)	196	200	202	205
TN(Malignant)	238	243	246	247
TN(Without Tumor)	212	213	216	218
FN(Benign)	10	06	03	02
FN(Malignant)	10	08	05	02
FN(Without Tumor)	14	10	08	06

Figure-19: Different methods with TP,FP,TN and FN for Benign, Malignant tumor and without tumor

Parameters	Combined Wiener and Anisotropic Filter using CSA with Otsu as an Objective function	Combined Wiener and Anisotropic Filter using CSA with Kapur Entropy as an Objective function	Combined Wiener and Anisotropic Filter using CSA with Tsallis Entropy as an Objective function	Combined Wiener and Anisotropic Filter using CSA with Combined Otsu and Tsallis Entropy as an Objective function
Se(Benign Tumor)	0.92308	0.95385	0.97692	0.98462
Se(Malignant Tumor)	0.88889	0.91111	0.94444	0.97778
Se(Without Tumor)	0.88333	0.91667	0.93333	0.95000
Sp(Benign Tumor)	0.93333	0.95238	0.96190	0.97619
Sp(Malignant Tumor)	0.95200	0.97200	0.98400	0.98800
Sp(Without Tumor)	0.96363	0.96818	0.98181	0.99090
PPV(Benign Tumor)	0.89552	0.92537	0.94074	0.96241
PPV(Malignant Tumor)	0.86957	0.92135	0.95506	0.96703
PPV(Without Tumor)	0.92982	0.94017	0.96552	0.98276
NPV(Benign Tumor)	0.95145	0.97087	0.98536	0.99033
NPV(Malignant Tumor)	0.95967	0.96812	0.98000	0.99196
NPV(Without Tumor)	0.93805	0.95515	0.96428	0.97321
ACC(Benign Tumor)	0.92941	0.95294	0.96764	0.97941
ACC(Malignant Tumor)	0.93529	0.95588	0.97352	0.98529
ACC(Without Tumor)	0.93529	0.95000	0.96470	0.97647
ACC(all)	0.90000	0.92941	0.95294	0.97059

Figure-20: Performance evaluation statistical parameters for brain tumor classification using 3×3 Confusion Matrix

6) GUI Implementation

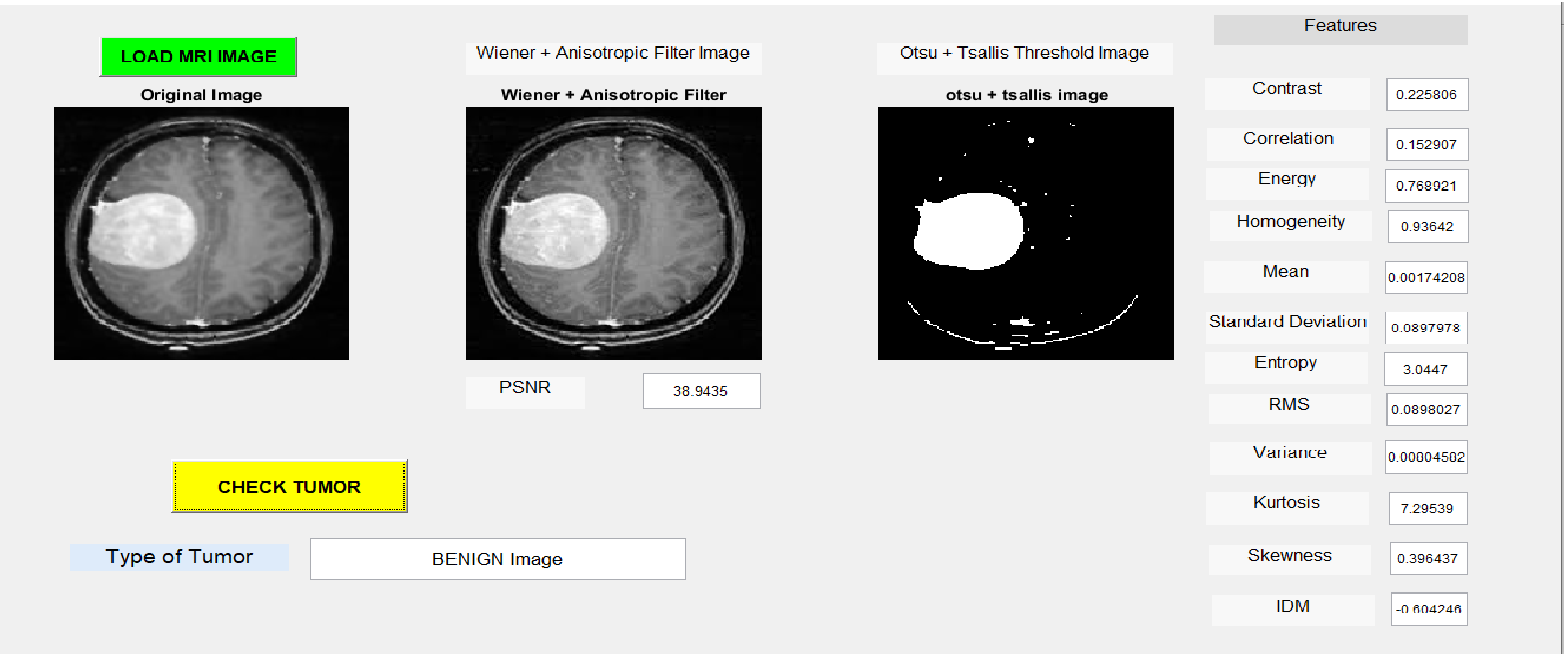

Figure-21: GUI Implementation of the tumor classification for Image-1

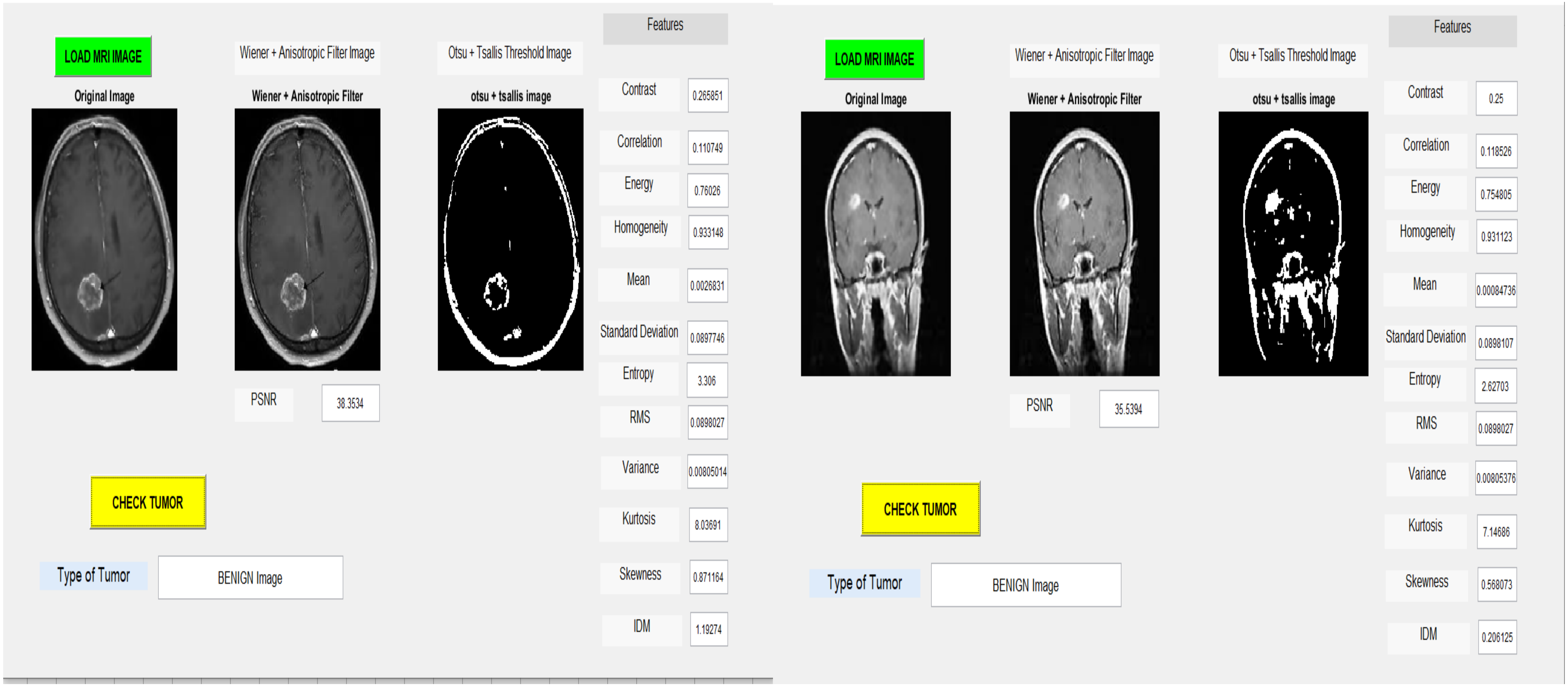

Figure-22: GUI Implementation of the tumor classification for different images

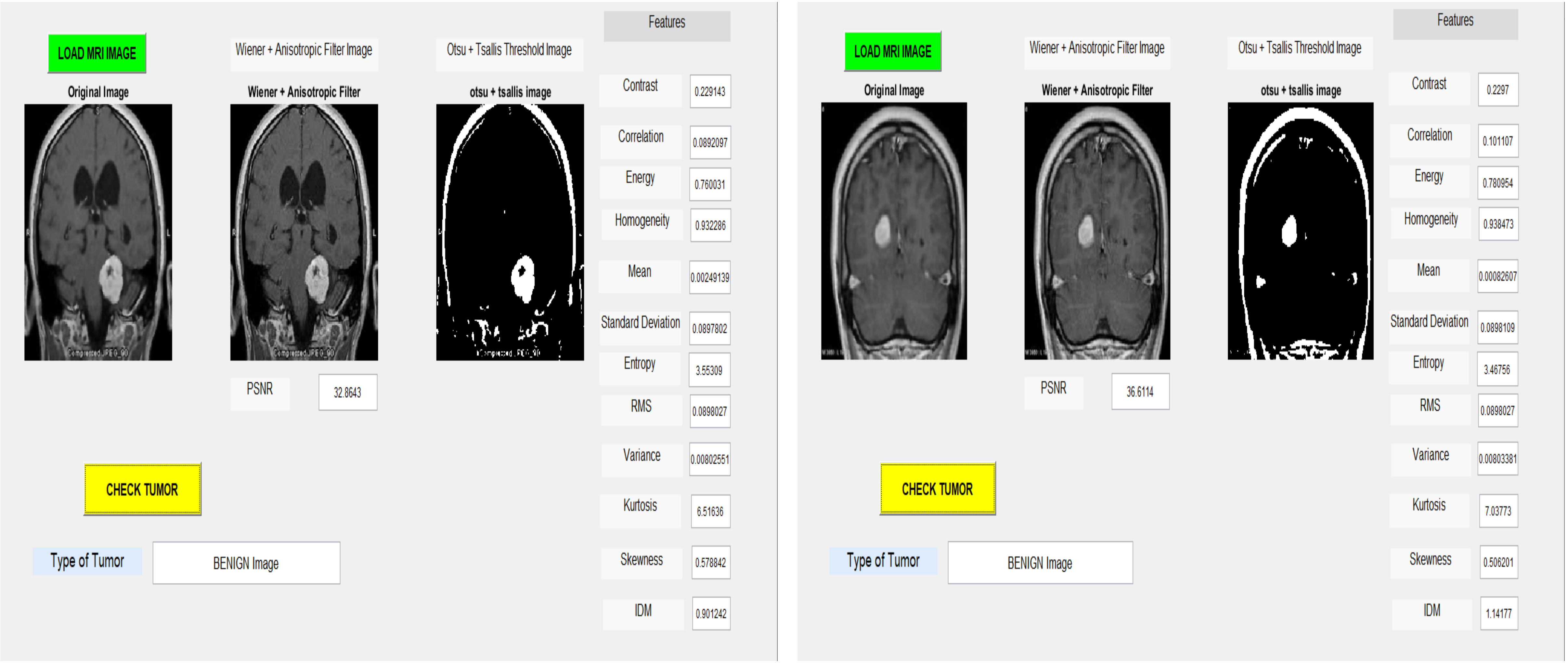

Figure-23: GUI Implementation of the tumor classification for different images

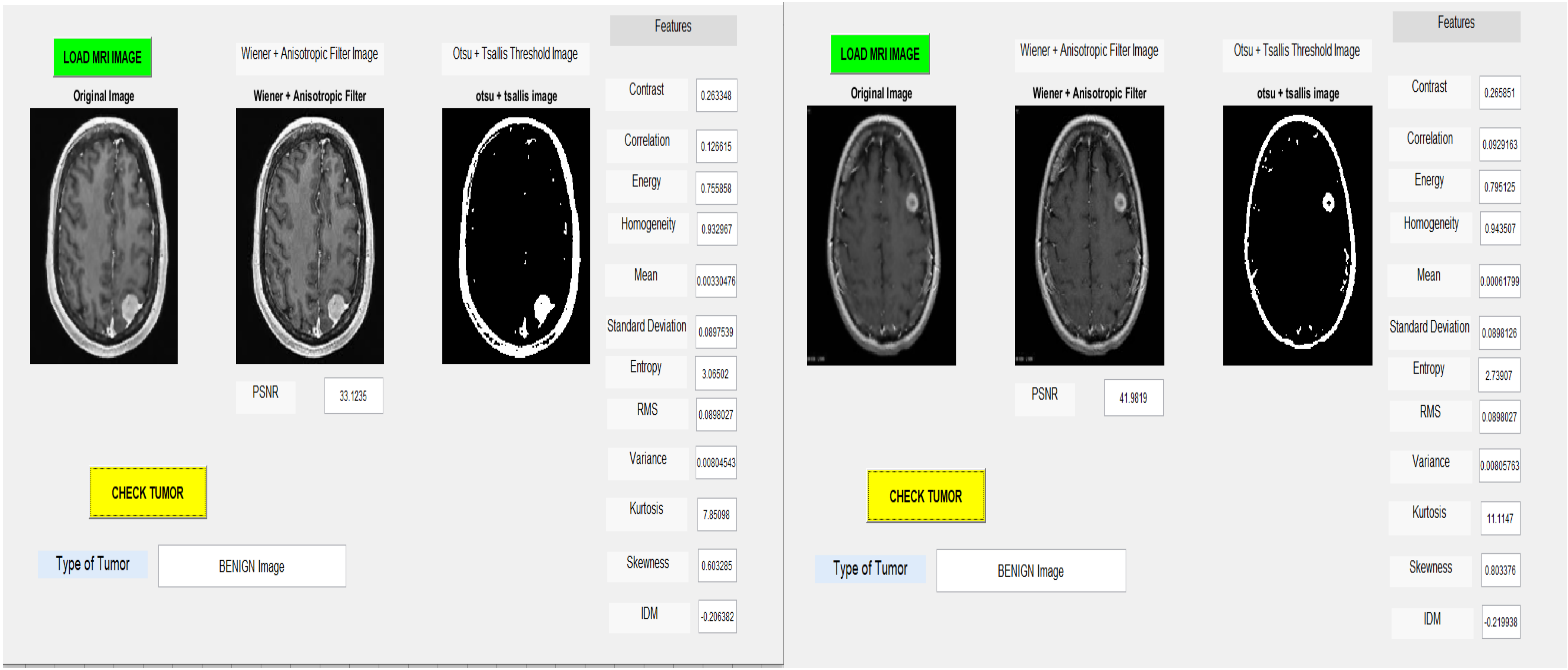

Figure-24: GUI Implementation of the tumor classification for different images

Figure-25: GUI Implementation of the tumor classification for different images

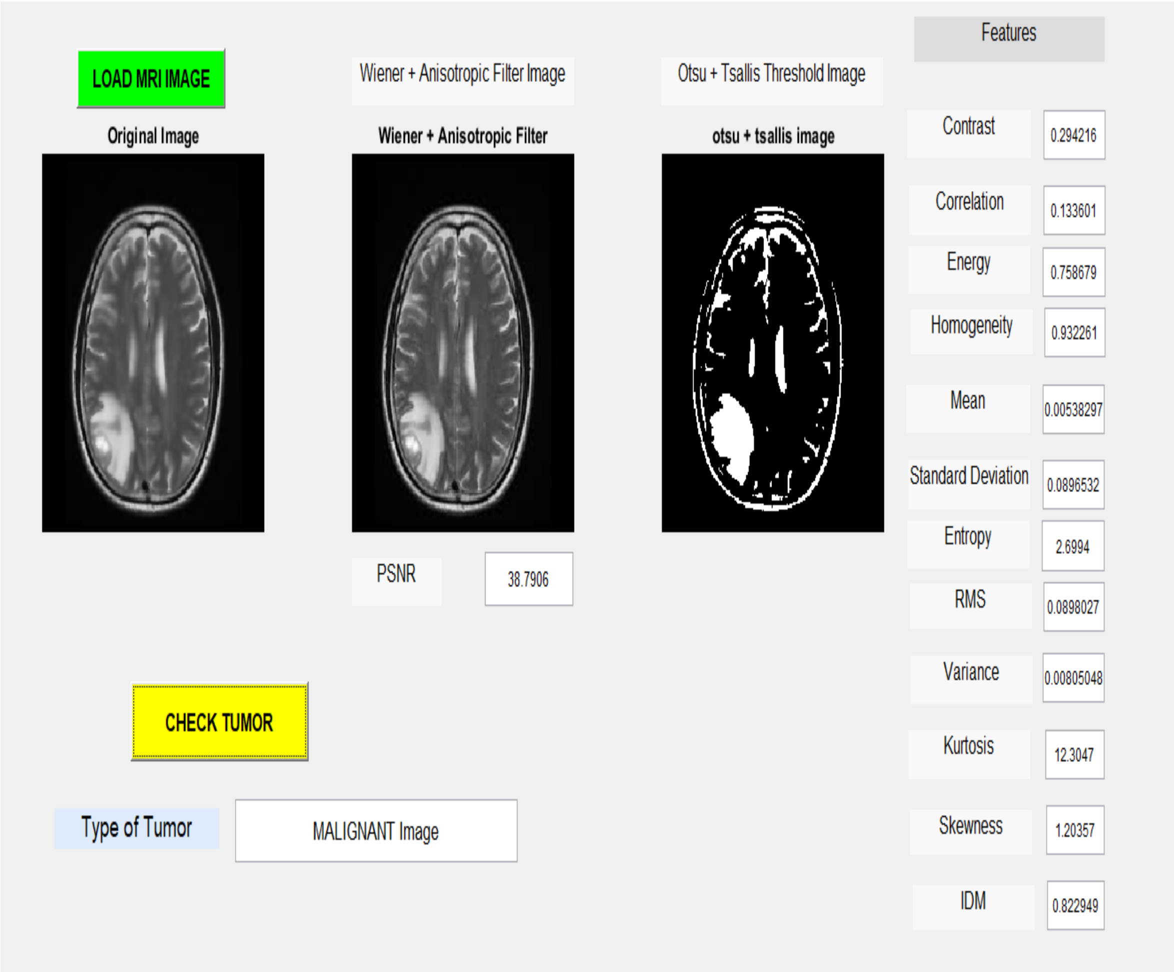

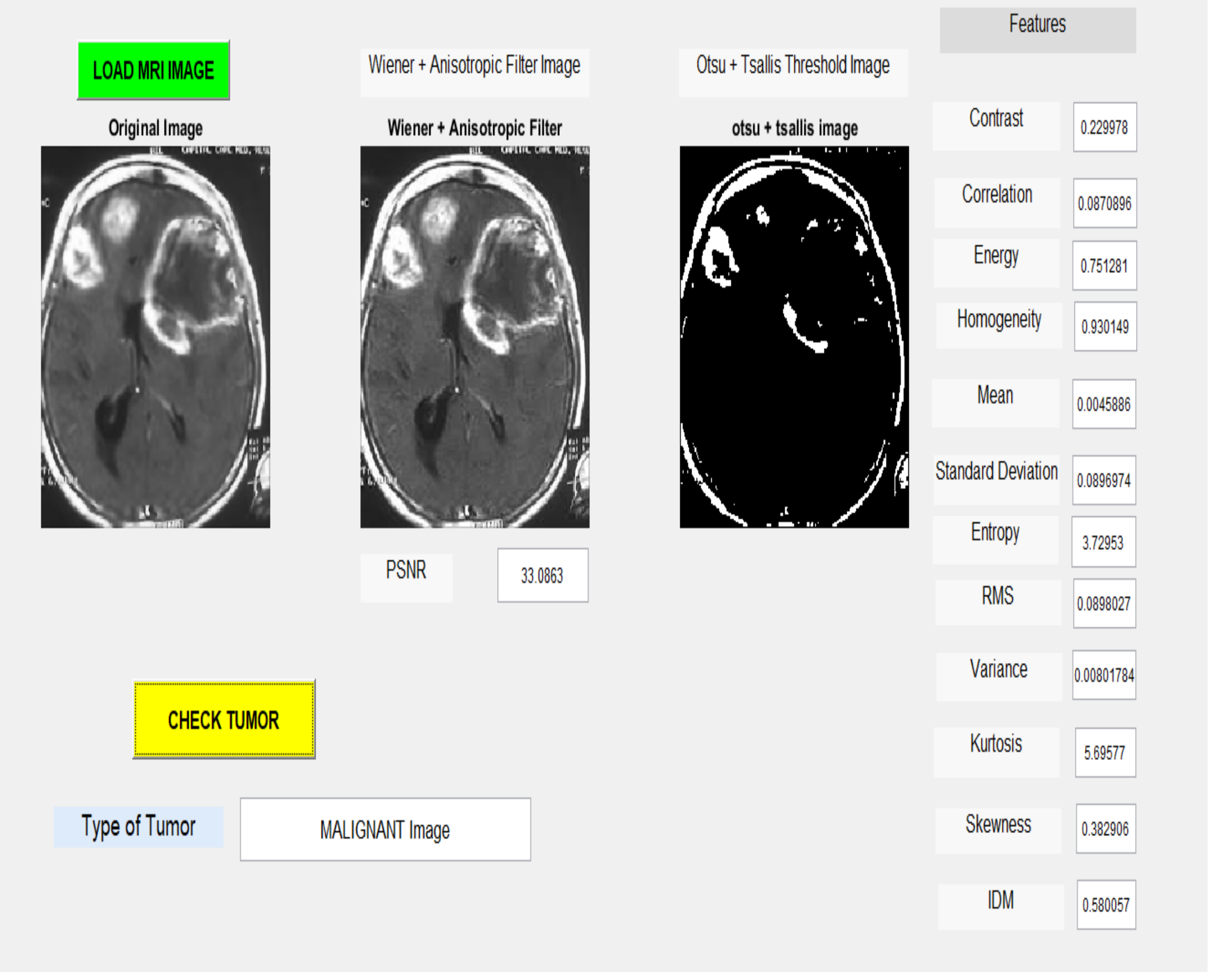

Figure-26: GUI Implementation of the tumor classification for different images

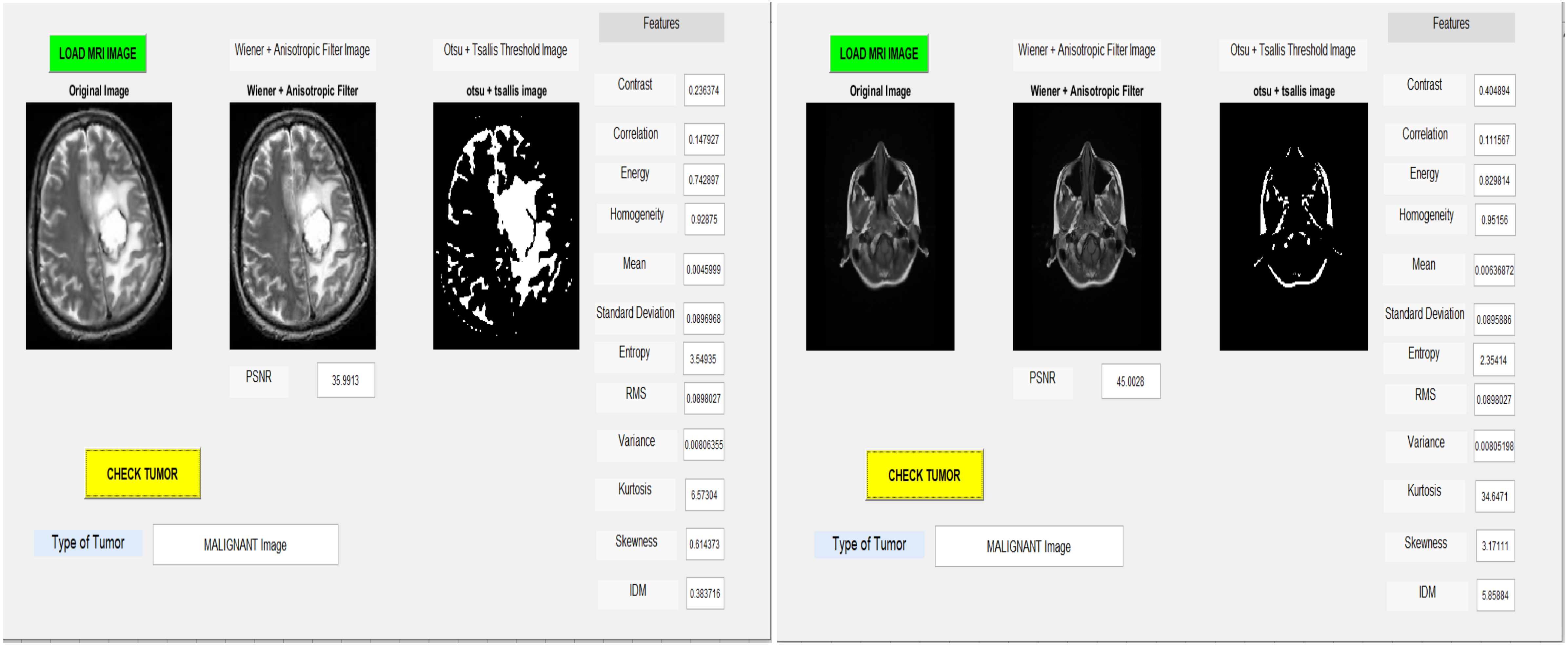

Figure-27: GUI Implementation of the tumor classification for different images

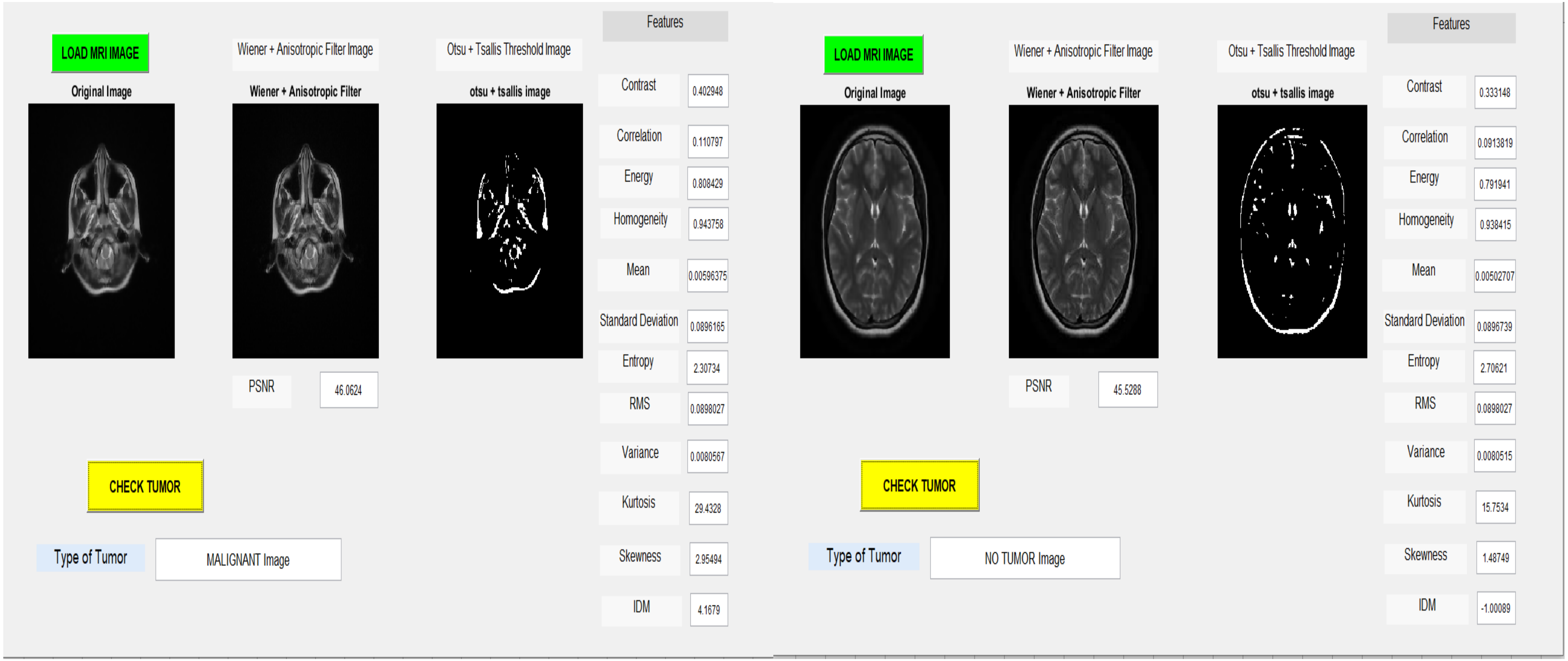

Figure-28: GUI Implementation of the tumor classification for different images

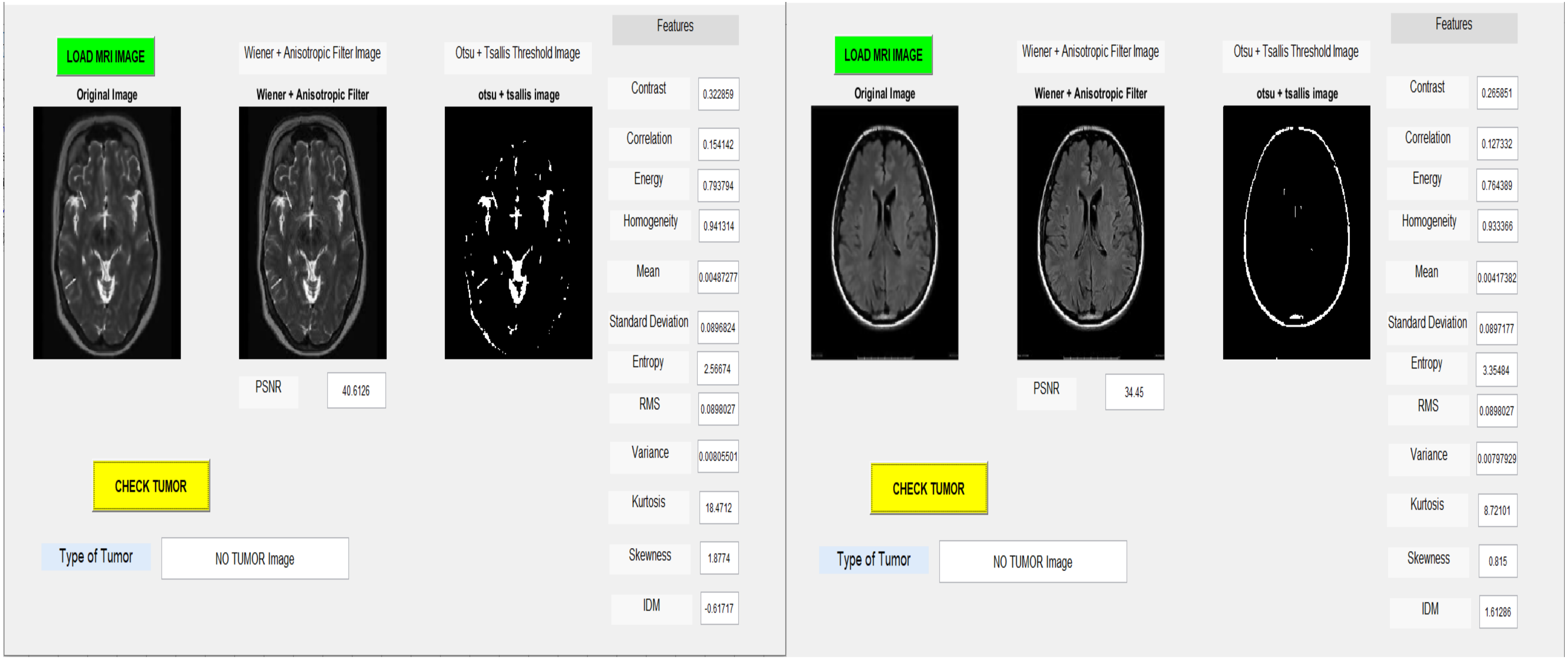

Figure-29: GUI Implementation of the tumor classification for different images

6) ACKNOWLEDGEMENT

I am very much thankful to the "**Sahyog Imaging Centre, SSG Hospital, Baroda Medical College, The Maharaja Sayajirao University of the Baroda, Vadodara, Gujarat, India"** was provided the patient data for the research work. Also thanks to the **Head, Department of the Radiologist, Prof. Chetan Mehta** and other professors of the Department of the Radiologist to help me for bifurcation and validation of the patients data.

7) CONCLUSION

- Dataset – Online kaggle dataset (www.kaggle.com) and Patients data from Sahyog Imaging Centre, SSG Hospital
- Pre-Processing - Wiener filter, Anisotropic filter, Median filter, Non-Local Means filter and Combined filters
  - Parameters - Peak Signal to Noise Ratio, Mean Square Error, Root Mean Square Error and Universal Quality Index
  - Combined Wiener and Anisotropic used for next stage.
- Segmentation - Cuckoo Search algorithm using different objective functions – Otsu’s, Kapur Entropy, Tsallis Entropy, Combined Otsu’s and Tsallis Entropy

- For Feature extraction – Discrete Wavelet Transform
    - Feature matrix is generated using twelve different parameters. Twelve statistical parameters covered are Contrast, Correlation, Energy, Homogeneity, Mean, Standard Deviation, Entropy, Root Mean Square, Variance, Kurtosis, Skewness and Inverse Different Moment
- Classification – Support vector machine
    - 2×2 and 3×3 confusion matrix
    - Statistical parameters - Sensitivity, Specificity, Positive Predictive Value, Negative Predictive Value and Accuracy
        - 2×2 confusion matrix - With Tumor or Without Tumor
        - 3×3 confusion matrix - Benign Tumor, Malignant Tumor and Without Tumor
- Cuckoo Search algorithm using Combined Otsu's and Tsallis Entropy gives better results compare to other algorithms.

8) FUTURE SCOPE

➢ Research work can be extended with following possibilities:

- More enhancement can be expressed with converting 2D data into 3D volumetric data
- More optimization can be achieved with trial of different hybrid algorithms

9) PUBLICATIONS

CONFERENCE PAPERS

[1] B. K. Pancholi and P. S. Modi, "Noise reduction in Clinical MRI Scans employing Filter Combining Techniques," 2022 2nd International Conference on Technological Advancements in Computational Sciences (ICTACS), Tashkent, Uzbekistan, 2022, pp. 474-480, doi: 10.1109/ICTACS56270.2022.9988482, ISBN : 978-1-6654-7658-4, EISBN : 978-1-6654-7657-7

[2] B. K. Pancholi, P. S. Modi and N. G. Chitaliya, “A Review of Noise Reduction Filtering Techniques for MRI Images”, 5th International Conference on Contemporary Computing and Informatics (IC3I-2022), Amity University, Greater Noida, Uttar Pradesh, pp. 954 - 960, doi: 10.1109/IC3I56241.2022.10073389, ISBN : 979-8-3503-9827-4, EISBN:979-8-3503-9826-7

JOURNAL PAPERS

[1] Bhavna Pancholi, Pramod Modi, Nehal Chitaliya, “Clasisifying MRI Images for Cerebral Tumor Using Soft Computing Techniques”, Proceedings on Engineering Sciences, Vol 5, no. 2, 2023, ISSN - 2620-2832, pp. 311-324. doi: 10.24874/PES05.02.014

[2] Bhavna Pancholi, Pramod Modi, Nehal Chitaliya, “The Development of A New Algorithm For Classifying Cerebral Tumors Using MRI Images”, Salud, Ciencia y Tecnologia, Vol 3, 2023, ISSN - 2796-9711, pp. 434-450. doi: 10.56294/saludcyt2023414

[3] Bhavna Pancholi, Pramod Modi, Nehal Chitaliya, “A novel multithresholding algorithm for segmentation of the MRI images”, Salud, Ciencia y Tecnologia, Vol 3, 2023, ISSN - 2796-9711, pp. 402-419. doi: 10.56294/saludcyt2023408

PATENT

[1] Pancholi B. et al. (2023). A System For Brain Tumor detection and method therefore (Indian Patent Application No. 202321003884), published 10-02-2023

ipindiaservices.gov.in/PatentSearch/PatentSearch/ViewApplicationStatus

Office of the Controller General of Patents, Designs & Trade Marks
Department of Industrial Policy & Promotion,
Ministry of Commerce & Industry,
Government of India

सत्यमेव जयते

INTELLECTUAL PROPERTY INDIA
PATENTS | DESIGNS | TRADE MARKS
GEOGRAPHICAL INDICATIONS

Application Details	
APPLICATION NUMBER	202321003884
APPLICATION TYPE	ORDINARY APPLICATION
DATE OF FILING	20/01/2023
APPLICANT NAME	**PANCHOLI, BHAVNA K (Faculty of Technology and Engineering, The Maharaja Sayajirao University of Baroda)**
TITLE OF INVENTION	"A SYSTEM FOR BRAIN TUMOR DETECTION AND METHOD THEREFORE."
FIELD OF INVENTION	BIO-MEDICAL ENGINEERING
E-MAIL (As Per Record)	iprmaulesh@outlook.com
ADDITIONAL-EMAIL (As Per Record)	iprmaulesh@gmail.com
E-MAIL (UPDATED Online)	
PRIORITY DATE	
REQUEST FOR EXAMINATION DATE	--
PUBLICATION DATE (U/S 11A)	10/02/2023

10) REFERENCES

[1] T. G. Devi, N. Patil, S. Rai, and C. S. Philipose, “Gaussian Blurring Technique for Detecting and Classifying Acute Lymphoblastic Leukemia Cancer Cells from Microscopic Biopsy Images,” Life, vol. 13, no. 2, 2023, doi: 10.3390/life13020348.

[2] A. V. P. Sarvari and K. Sridevi, “An optimized EBRSA-Bi LSTM model for highly undersampled rapid CT image reconstruction,” Biomed. Signal Process. Control, vol. 83, no. December 2022, p. 104637, 2023, doi: 10.1016/j.bspc.2023.104637.

[3] M. A. Talukder et al., “An efficient deep learning model to categorize brain tumor using reconstruction and fine-tuning,” Expert Syst. Appl., vol. 230, no. August 2022, p. 120534, 2023, doi: 10.1016/j.eswa.2023.120534.

[4] S. A. Lakshmi and K. Anandavelu, “Enhanced Cuckoo Search Optimization Technique for Skin Cancer Diagnosis Application,” Intell. Autom. Soft Comput., vol. 35, no. 3, pp. 3403–3413, 2023, doi: 10.32604/iasc.2023.030970.

[5] J. Amin, M. Sharif, A. Haldorai, M. Yasmin, and R. S. Nayak, “Brain tumor detection and classification using machine learning: a comprehensive survey,” *Complex Intell. Syst.*, vol. 8, no. 4, pp. 3161–3183, 2022, doi: 10.1007/s40747-021-00563-y.

[6] S. Minaee, Y. Boykov, F. Porikli, A. Plaza, N. Kehtarnavaz, and D. Terzopoulos, “Image Segmentation Using Deep Learning: A Survey,” IEEE Trans. Pattern Anal. Mach. Intell., vol. 44, no. 7, pp. 3523–3542, 2022, doi: 10.1109/TPAMI.2021.3059968.

[7] F. A. Hashim, E. H. Houssein, K. Hussain, M. S. Mabrouk, and W. Al-Atabany, “Honey Badger Algorithm: New metaheuristic algorithm for solving optimization problems,” Math. Comput. Simul., vol. 192, pp. 84–110, 2022, doi: 10.1016/j.matcom.2021.08.013.

[8] A. Sharma and V. Chaurasia, “MRI denoising using advanced NLM filtering with non-subsampled shearlet transform,” *Signal, Image Video Process.*, vol. 15, no. 6, pp. 1331–1339, 2021, doi: 10.1007/s11760-021-01864-y.

[9] K. Huang and H. Zhu, “Image Noise Removal Method Based on Improved Nonlocal Mean Algorithm,” Complexity, vol. 2021, 2021, doi: 10.1155/2021/5578788.

[10] E. H. Houssein, B. E. din Helmy, D. Oliva, A. A. Elngar, and H. Shaban, “A novel Black Widow Optimization algorithm for multilevel thresholding image segmentation,” Expert Syst. Appl., vol. 167, p. 114159, 2021, doi: 10.1016/j.eswa.2020.114159.

[11] J. Rahaman and M. Sing, “An efficient multilevel thresholding based satellite image segmentation approach using a new adaptive cuckoo search algorithm,” Expert Syst. Appl., vol. 174, no. January, p. 114633, 2021, doi: 10.1016/j.eswa.2021.114633.

[12] L. C. C. Yogendra Kumar, By, S. Date, P. Date, C. Verma, C. S. Algorithm, and O. Problems, “A survey on Cuckoo Search Algorithm for Optimization Problems A survey on Cuckoo Search Algorithm for Optimization Problems,” no. August, pp. 0–16, 2021, doi: 10.36227/techrxiv.14199221.

[13] S. K. Dinkar, K. Deep, S. Mirjalili, and S. Thapliyal, “Opposition-based Laplacian Equilibrium Optimizer with application in Image Segmentation using Multilevel Thresholding,” Expert Syst. Appl., vol. 174, no. February, p. 114766, 2021, doi: 10.1016/j.eswa.2021.114766.

[14] L. Duan, S. Yang, and D. Zhang, “Multilevel thresholding using an improved cuckoo search algorithm for image segmentation,” J. Supercomput., vol. 77, no. 7, pp. 6734–6753, 2021, doi: 10.1007/s11227-020-03566-7.

[15] R. Zheng, “An Improved Cuckoo Search Algorithm,” ICSAI 2021 - 7th Int. Conf. Syst. Informatics, vol. 2021, 2021, doi: 10.1109/ICSAI53574.2021.9664073.

[16] S. Widiyanto, Y. Sukra, S. Madenda, D. T. Wardani, and E. P. Wibowo, “Texture feature extraction based on GLCM and DWT for beef tenderness classification,” Proc. 3rd Int. Conf. Informatics Comput. ICIC 2018, no. February 2021, pp. 1–4, 2018, doi: 10.1109/IAC.2018.8780569

[17] P. Sharma and A. P. Shukla, A Review on Brain Tumor Segmentation and Classification for MRI Images, no. Mi. Multimedia Tools and Applications, 2021. doi: 10.1109/ICACITE51222.2021.9404662.

[18] Chahal, Prabhjot Kaur, et al. “A Survey on Brain Tumor Detection Techniques for MR Images.” Multimedia Tools and Applications, vol. 79, no. 29-30, 11 May 2020, pp. 21771–21814, 10.1007/s11042-020-08898-3.

[19] A. Shankar, J. Bomanji, and H. Hyare, “Hybrid pet–MRI imaging in paediatric and tya brain tumours: Clinical applications and challenges,” J. Pers. Med., vol. 10, no. 4, pp. 1–19, 2020, doi: 10.3390/jpm10040218.

[20] V. Sawlani et al., “Multiparametric MRI: practical approach and pictorial review of a useful tool in the evaluation of brain tumours and tumour-like lesions,” Insights Imaging, vol. 11, no. 1, pp. 1–19, 2020

[21] P. K. Chahal, S. Pandey, and S. Goel, “A survey on brain tumor detection techniques for MR images,” Multimed. Tools Appl., vol. 79, no. 29–30, pp. 21771–21814, 2020, doi: 10.1007/s11042-020-08898-3.

[22] D M Mahalakshmi and S Sumathi, “Performance Analysis of Svm and Deep Learning With Cnn for Brain Tumor Detection and Classification,” ICTACT J. Image Video Process. , vol. 10, no. 03, pp. 2145–2152, 2020, doi: 10.21917/ijivp.2020.0307.

[23] C. J. J. Sheela and G. Suganthi, “An efficient denoising of impulse noise from MRI using adaptive switching modified decision based unsymmetric trimmed median filter,” Biomed. Signal Process. Control, vol. 55, p. 101657, 2020, doi: 10.1016/j.bspc.2019.101657.

[24] P. Sagar, A. Upadhyaya, S. K. Mishra, R. N. Pandey, S. S. Sahu, and G. Panda, “A circular adaptive median filter for salt and pepper noise suppression from MRI images,” J. Sci. Ind. Res. (India)., vol. 79, no. 10, pp. 941–944, 2020, doi: 10.56042/jsir.v79i10.43588.

[25] A. Noor, Y. Zhao, R. Khan, L. Wu, and F. Y. O. Abdalla, “Median filters combined with denoising convolutional neural network for Gaussian and impulse noises,” Multimed. Tools Appl., vol. 79, no. 25–26, pp. 18553–18568, 2020, doi: 10.1007/s11042-020-08657-4.

[26] G. Theaud, J. C. Houde, A. Boré, F. Rheault, F. Morency, and M. Descoteaux, “TractoFlow: A robust, efficient and reproducible diffusion MRI pipeline leveraging Nextflow & Singularity,” Neuroimage, vol. 218, 2020, doi: 10.1016/j.neuroimage.2020.116889.

[27] R. Kalpana and P. Chandrasekar, “An optimized technique for brain tumor classification and detection with radiation dosage calculation in MR image,” Microprocess. Microsyst., vol. 72, p. 102903, 2020, doi: 10.1016/j.micpro.2019.102903.

[28] R. Srikanth, “Spontaneous Coronary Artery Dissection: Failure of the Conservative Strategy Due to Predominance of the False Lumen,” JACC Cardiovasc. Interv., vol. 10, no. 15, pp. e139–e140, 2020, doi: 10.1016/j.jcin.2017.04.032.

[29] A. Das, S. Agrawal, L. Samantaray, R. Panda, and A. Abraham, “State-of-the art optimal multilevel thresholding methods for brain MR image analysis,” Rev. d’Intelligence Artif., vol. 34, no. 3, pp. 243–256, 2020, doi: 10.18280/ria.340302.

[30] C. L. Chowdhary and D. P. Acharjya, “Segmentation and Feature Extraction in Medical Imaging: A Systematic Review,” Procedia Comput. Sci., vol. 167, no. 2019, pp. 26–36, 2020, doi: 10.1016/j.procs.2020.03.179.

[31] P. P. Gumaste and V. K. Bairagi, “A hybrid method for brain tumor detection using advanced textural feature extraction,” Biomed. Pharmacol. J., vol. 13, no. 1, pp. 145–157, 2020, doi: 10.13005/bpj/1871.

[32] S. Vani Kumari and K. Usha Rani, “Analysis on Various Feature Extraction Methods for Medical Image Classification,” no. July, pp. 19–31, 2020, doi: 10.1007/978-3-030-46943-6_3.

[33] S. Anandh, R. Vasuki, and Y. P. Rachelin, “New efficient kNN classifier to detect abdominal aortic aneurysms using digital image processing,” Int. J. Adv. Res. Eng. Technol., vol. 11, no. 5, pp. 52–64, 2020, doi: 10.34218/IJARET.11.5.2020.007.

[34] M. Shakunthala and K. Helenprabha, “Preprocessing Analysis of Brain,” 2019 IEEE Int. Conf. Electr. Comput. Commun. Technol., pp. 1–5, 2019

[35] M. Gao, B. Kang, X. Feng, W. Zhang, and W. Zhang, “Anisotropic diffusion based multiplicative speckle noise removal,” Sensors (Switzerland), vol. 19, no. 14, pp. 44–46, 2019, doi: 10.3390/s19143164.

[36] O. Tarkhaneh and H. Shen, “An adaptive differential evolution algorithm to optimal multi-level thresholding for MRI brain image segmentation,” Expert Syst. Appl., vol. 138, 2019, doi: 10.1016/j.eswa.2019.07.037.

[37] F. A. Bohani et al., “Multilevel thresholding of brain tumor MRI images: Patch-Levy Bees Algorithm versus Harmony Search Algorithm,” Int. J. Electr. Comput. Eng. Syst., vol. 10, no. 2, pp. 45–57, 2019, doi: 10.32985/ijeces.10.2.1.

[38] W. Ayadi, W. Elhamzi, I. Charfi, and M. Atri, “A hybrid feature extraction approach for brain MRI classification based on Bag-of-words,” Biomed. Signal Process. Control, vol. 48, pp. 144–152, 2019, doi: 10.1016/j.bspc.2018.10.010.

[39] K. Jadwa Assist, “Wiener Filter based Medical Image De-noising,” Int. J. Sci. Eng. Appl., vol. 7, no. 09, pp. 318–323, 2018, [Online]. Available: www.ijsea.com318

[40] Anchal, S. Budhiraja, B. Goyal, A. Dogra, and S. Agrawal, “An efficient image denoising scheme for higher noise levels using spatial domain filters,” Biomed. Pharmacol. J., vol. 11, no. 2, pp. 625–634, 2018, doi: 10.13005/bpj/1415.

[41] R. Sumathi, M. Venkatesulu, and S. P. Arjunan, “Extracting tumor in MR brain and breast image with Kapur’s entropy based Cuckoo Search Optimization and morphological reconstruction filters,” Biocybern. Biomed. Eng., vol. 38, no. 4, pp. 918–930, 2018, doi: 10.1016/j.bbe.2018.07.005.

[42] T. Çevik, A. Mustafa, and N. Çevik, “A Comprehensive Performance Analysis of GLCM-DWT-based Classification on Fingerprint Identification,” Int. J. Comput. Appl., vol. 180, no. 32, pp. 42–47, 2018, doi: 10.5120/ijca2018916909.

[43] M. Khalil, H. Ayad, and A. Adib, “Performance evaluation of feature extraction techniques in MR-Brain image classification system,” Procedia Comput. Sci., vol. 127, pp. 218–225, 2018, doi: 10.1016/j.procs.2018.01.117.

[44] D. Jha, J. I. Kim, M. R. Choi, and G. R. Kwon, “Pathological Brain Detection Using Weiner Filtering, 2D-Discrete Wavelet Transform, Probabilistic PCA, and Random Subspace Ensemble Classifier,” Comput. Intell. Neurosci., vol. 2017, 2017, doi: 10.1155/2017/4205141.

[45] E. Yilmaz, T. Kayikcioglu, and S. Kayipmaz, “Noise removal of CBCT images using an adaptive anisotropic diffusion filter,” 2017 40th Int. Conf. Telecommun. Signal Process. TSP 2017, vol. 2017-January, pp. 650–653, 2017, doi: 10.1109/TSP.2017.8076067.

[46] M. H. Mozaffari and W. S. Lee, “Convergent heterogeneous particle swarm optimisation algorithm for multilevel image thresholding segmentation,” IET Image Process., vol. 11, no. 8, pp. 605–619, 2017, doi: 10.1049/iet-ipr.2016.0489.

[47] M. Fatimaezzahra, B. Loubna, S. Mohamed, and E. Abdelaziz, “A combined cuckoo search algorithm and genetic algorithm for parameter optimization in computer vision,” Int. J. Appl. Eng. Res., vol. 12, no. 22, pp. 12940–12954, 2017.

[48] A. S. Joshi, O. Kulkarni, G. M. Kakandikar, and V. M. Nandedkar, “Cuckoo Search Optimization- A Review,” Mater. Today Proc., vol. 4, no. 8, pp. 7262–7269, 2017, doi: 10.1016/j.matpr.2017.07.055.

[49] J. Xu, Y. Jia, Z. Shi, and K. Pang, “An improved anisotropic diffusion filter with semi-adaptive threshold for edge preservation,” Signal Processing, vol. 119, pp. 80–91, 2016, doi: 10.1016/j.sigpro.2015.07.017.

[50] M. Dhieb and M. Frikha, “Image Segmentation Based on Particle,” 2016.

[51] J. Yang, J. Fan, D. Ai, S. Zhou, S. Tang, and Y. Wang, “Brain MR image denoising for Rician noise using pre-smooth non-local means filter,” Biomed. Eng. Online, vol. 14, no. 1, pp. 1–20, 2015, doi: 10.1186/1475-925X-14-2.

[52] P. Mohapatra, S. Chakravarty, and P. K. Dash, “An improved cuckoo search based extreme learning machine for medical data classification,” Swarm Evol. Comput., vol. 24, pp. 25–49, 2015, doi: 10.1016/j.swevo.2015.05.003.

[53] Yang, Xin-She, and Suash Deb. “Cuckoo Search via Lévy Flights.” IEEE Xplore, 1 Dec. 2009, ieeexplore.ieee.org/document/5393690.

Thanks